2009

Genipin-crosslinked electrospun collagen nanofibers

Mina Mekhail

Genipin-crosslinked electrospun collagen nanofibers

(Spine title: Genipin-crosslinked electrospun collagen nanofibers)

(Thesis format: Monograph)

by

Mina Mekhail

Graduate Program in Biomedical Engineering

A thesis submitted in partial fulfillment of the requirements for the degree of Master in Engineering Science

The School of Graduate and Postdoctoral Studies

The University of Western Ontario

London, Ontario, Canada

Abstract

Tissue engineering deals with creating tissues, using patient-derived cells, in order to restore, maintain or improve existing tissue function. In traditional tissue engineering, tissues are grown in-vitro prior to insertion in the body, and thus a scaffold is needed to support and guide the cells during growth. Nanofibrous scaffolds are considered promising since they mimic the extracellular matrix, have a high surface area-to-volume ratio, and possess excellent porosity and pore interconnectivity. In this research collagen type I nanofibers were fabricated using electrospinning. Collagen nanofibers were unstable in aqueous environments, and thus crosslinking was required. Glutaraldehyde, which is cytotoxic to cells, is currently the chemical crosslinking agent used by most research groups to stabilize collagen nanofibers. In this thesis, a novel approach, using genipin (a natural crosslinking agent), was introduced to crosslink the electrospun collagen nanofibers. Genipin has been proven to be significantly less cytotoxic compared to glutaraldehyde.

Keywords: Tissue engineering, electrospinning, nanofibers, collagen, genipin, crosslinking

Acknowledgments

This thesis would have not been possible without the guidance and support of my supervisor, Dr. Wankei Wan. His words of wisdom and motivation, usually during coffee breaks, were both invaluable and assuring.

I would also like to acknowledge: Ken Wong, for teaching me how to electrospin, and for spending many hours acquiring Scanning Electron Microscopy images of my nanofibers; Donna Padavan, for assisting me in acquiring the Fourier-Transform Infrared spectra of my samples, and also for lending me many of her glassware; Andrew Norman, for being the good friend he is, and for providing the beer during times of frustration; and everyone else in Dr. Wan's lab, for their help and support in, and out of, the lab.

I would like to thank Dr. David O'Gorman for granting me access to the cell-culturing facility in his lab, and for taking the time to help me interpret some of my cell seeding results. A special thanks goes to Dr. Yan Wu and Linda Vi for teaching me cell seeding, cell staining and cell imaging using fluorescence microscopy.

Wholehearted thanks goes to my family, for their love and care, which were the source of energy that kept me going throughout my Masters degree. Finally, I thank God for giving me the perseverance and patience to complete this project.

Table of Contents

List of Figures

List of Tables

1 Introduction

The term 'tissue engineering' was first introduced during a bioengineering panel meeting at the US National Science Foundation (NSF) in 1987. The following year, the definition of tissue engineering was established during a NSF-funded workshop as *"an interdisciplinary field that applies the principles of engineering and life sciences towards the development of biological substitutes that restore, maintain or improve tissue function"* [1].

Although it was not till 1987 that the definition was created, tissue engineering was practiced long before then. One of the earliest references to tissue engineering was a painting by Fra Angelica, in 1440, called 'The Healing of Justinian'; in it, saints Damien and Cosmos were depicted attaching a homograft leg to a wounded soldier [2]. The beginning of tissue engineering, as we know it today, was in the early 1970s when Dr. W.T. Green, a pediatric orthopedic surgeon at the Boston Children's Hospital, attempted to generate new cartilage by seeding chondrocytes on bone spicules and inserting the constructs into nude mice. Although he was unsuccessful, he predicted the need to fabricate biocompatible scaffolds and seed them with cells to generate new tissue. Consequently, during the 1980s and early 1990s, various researchers were already working on regenerating skin, encapsulating cells and tissue engineering blood vessels [1]. All previous researchers were using the idea of a 'scaffold' material, they all used naturally occurring extracellular matrix (i.e. acellularized tissue) with chemical and physical properties that could not be manipulated. Joseph Vacanti and Robert Langer were of the first to introduce a scaffolding material with controlled properties. They designed branching networks of synthetic biodegradable/biocompatible polymers [2]. Currently, both synthetic and natural biomaterials are being used to fabricate scaffolds for different applications, such as wound healing and tissue engineering. Many researchers prefer synthetic polymers due to their unparalleled tunability. However, new technologies have emerged to allow better tunability of natural polymers, thus a paradigm shift towards extracellular matrix polymers is taking place [3]. In this thesis, a natural polymer was used to fabricate the scaffold. The biomaterial used was Collagen type I, which is the most abundant protein in the body.

Traditional tissue engineering, as practiced by most researchers, involves the fabrication of a scaffold that contains growth factors (i.e. proteins that stimulate cells to proliferate, migrate and/or differentiate), and seeding the scaffolds with patient-derived cells (e.g. autologous adult stem cells). Cellular proliferation, differentiation and arrangement in the scaffold are then controlled using custom-built bioreactors. Regenerated tissue is then applied to the damaged or diseased area of the body to restore, maintain or improve tissue function [2].

Scaffolds, previously designed only to provide physical support to cells, are now being designed to mimic the mechanical, chemical and biological aspects of the native extracellular matrix (ECM). Researchers are realizing that three-dimensional (3D) scaffolds allow better cell growth and attachment compared to two-dimensional (2D) scaffolds, since they better mimic the ECM of native tissues [4]. In addition, an ideal 3D scaffold should possess certain characteristics, such as: (1) Biocompatibility, (2) Mechanical strength to provide physical support to cells, (3) Bioactivity to stimulate cell attachment, migration, proliferation and orientation, (4) Interconnected pores to allow cell migration into the scaffold and to allow the flow of nutrients into and wastes out of the scaffold, and (5) Biodegradability (with non-toxic byproducts) at a similar rate to tissue formation, [4].

One of the current popular approaches is the fabrication and application of 3D nanofibrous scaffolds. The scientific community defines nanofibers as fibers with diameters of 100 nm or less. However, the commercial sector considers fibers with diameters less than 500 nm as nanofibers [5]. Nanofibrous scaffolds are considered the most ideal in tissue engineering applications, since they: (1) Mimic the native extracellular matrix, (2) Provide a high surface area to volume ratio that allows for better cell attachment, and (3) Provide high porosity and pore-interconnectivity [5].

Therefore, based on the promising characteristics of nanofibers, the main objectives of this research were to: (1) Fabricate a three dimensional type I collagen nanofibrous scaffold via electrospinning, (2) Stabilize the scaffold in aqueous environments using a natural crosslinking agent called genipin, (3) Characterize the fibers

morphology before and after exposure to an aqueous environment, and (4) Examine the scaffold's cell compatibility.

The novelty of this research lies in the use of genipin to crosslink electrospun collagen nanofibers. A great deal of time was spent optimizing the crosslinking process. Genipin has been proven to be ~10,000 times less cytotoxic compared to the widely-used glutaraldehyde. Therefore, the potential use of genipin, as a chemical crosslinking agent, to stabilize electrospun collagen nanofibers is considered a significant improvement over the currently used glutaraldehyde. Successful crosslinking was achieved when the nanofibrous morphology of the scaffold was maintained after exposure to an aqueous environment for up to 7 days. Fiber morphology and swelling were studied after crosslinking and after exposure to the cell growth media. The degree of crosslinking and degradation were measured using the ninhydrin assay. The chemical compositions of crosslinked samples were studied using Fourier-Transform Infrared spectroscopy (FTIR). Finally, primary human fibroblasts were seeded on the scaffold and cellular attachment and morphology were studied.

2 Background and literature review

2.1 Electrospinning

Electrospinning (electrostatic spinning) is a method of producing polymeric nanofibers by introducing a liquid jet, containing a polymer, into an electric field through a millimeter diameter nozzle [6, 7]. A conventional electrospinning setup is composed of a syringe with a metallic needle, a syringe pump, a high voltage power supply and a metal collector (Figure 1). The polymer is either melted or dissolved in a solvent, and then fed into the syringe. The syringe is placed on a syringe pump and the solution is delivered at a controlled flow rate. An electric field is created by grounding the needle and charging the collector or vice versa. The induced electric field causes charging of the solution. At a specific voltage, when the electrostatic force exceeds the surface tension of the liquid droplet at the tip of the needle, a Taylor's cone is formed and the polymeric jet is ejected (Figure 2) [6, 7]. At low electric fields, the jet travels in a straight line and deposits on the collector. However, at high electric fields the polymeric jet first travels in a straight line, and then undergoes chaotic bending called 'whipping instability'. This instability speeds up the solvent evaporation rate, and deposits the polymer on the collector as dry, randomly oriented fibers. Shin et al. used high speed photography to demonstrate that the chaotic whipping grows wider, in a conical form, as the jet travels towards the collector [6]. The whipping instability is responsible for reducing the fiber diameters from micrometers to nanometers due to the stretching of the polymeric jet [6].
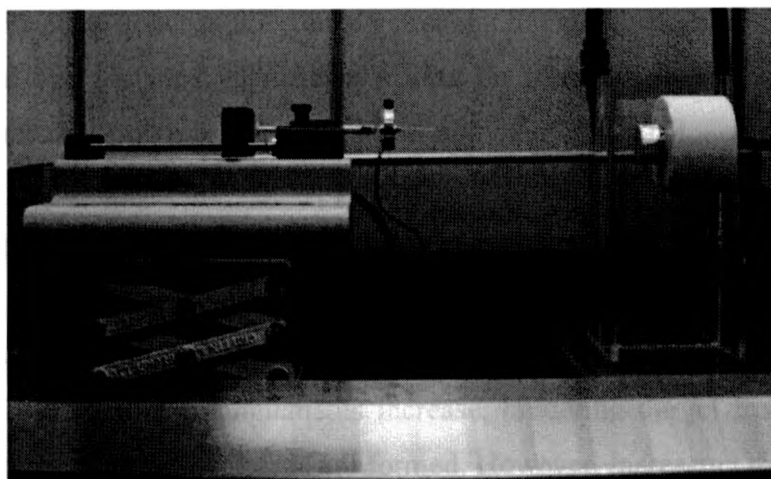
Figure 1. The electrospinning setup used in our lab
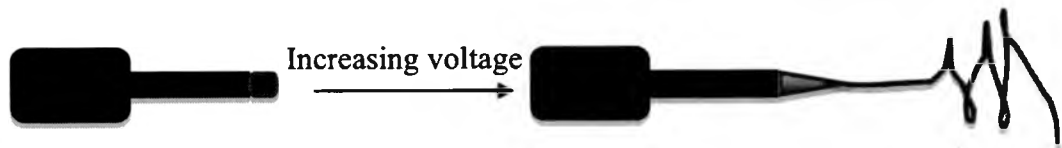
Figure 2. Effect of voltage increase on creating a Taylor's cone and ejecting a polymeric jet

Although the requirements for electrospinning nanofibers seem simple, in reality there are many parameters that affect fiber formation and final morphology. The main parameters can be divided into process parameters and solution parameters (Table 1).

Table 1. The two groups of electrospinning parameters

Solution parameters	Process parameters
Viscosity	Voltage
Surface tension	Tip-to-Collector distance
Conductivity	Feed-rate
	Orifice diameter
	Type of collector

2.1.1 Solution parameters

Solution parameters affect the final fibers' morphology, diameters and bead formation (defects in the fibers).

2.1.1.1 Viscosity

Polymer concentration and molecular weight (MW) are the two factors that affect the viscosity of the solution. Cui et al. performed an orthogonal experimental design to analyze the correlation between different electrospinning variables and found that the two parameters that had the most significant effects on fiber diameters and percent bead formation were the polymer concentration and the MW [8]. At low polymer concentrations the fibers do not dry before reaching the collector, and therefore contain a high percentage of beads; this is attributed to the inadequacy in the amount of polymer entanglements available [8]. Polymer entanglements are essential since they prevent the electrically charged jet from breaking up during electrospinning. As the polymer concentration is increased, entanglements increase, hindering the jet from breaking off and thus smooth fibers with few beads are formed. However, increasing the concentration above a certain limit will inhibit electrospinning due to high cohesiveness in the solution

[8]. The MW represents the length of a linear polymer chain, and thus a high MW means a longer polymer chain. Longer polymer chains will cause more entanglements, which in turn increases viscosity. Consequently, increasing the MW will increase fiber diameters and reduce bead formation. Electrospinning polymers with short branched chains are unfeasible, due to the lower number of entanglements and lower hydrodynamic radiuses as compared to linear polymers. However, highly branched poly(urethane urea)s have been successfully electrospun at high concentrations, compared to the linear chains. A high concentration was needed to increase entanglements due to the low hydrodynamic radius possessed by these branched polymers (even though the MW of the branched polymers was higher than its linear counterpart) [9, 10]. However, as is the case with polymeric concentration, increasing the MW beyond a certain limit will prohibit electrospinning. Therefore, it can be concluded that at a specific range of polymer concentrations and MWs electrospun fibers can be obtained with no beads and with nanometer diameters. This range is dependant on the type and properties of polymer used [5].

2.1.1.2 Surface Tension

Solvent molecules attract each other via intermolecular forces and each molecule in the solvent is pulled from all directions, thus the net force on the solvent molecule inside a solution is zero. However, the molecules on the surface are pulled into the solution, away from the surface, by the molecules deep in the liquid and weaker forces from the air molecules, therefore are exposed to a net force into the solution [5]. This causes the surface to be under tension and the phenomena is called surface tension.

Surface tension is responsible for the formation of a stable jet as well as the occurrence of beads [5]. At the instant the electrostatic force overcomes the surface tension of the liquid molecules, a charged jet forms. However, solutions with high surface tensions cause the jet to break and droplets to form instead. Decreasing the surface tension allows the formation of fibers with no beads [5].

2.1.1.3 Solution Conductivity

Stretching of the jet takes place due to the repulsion of the charges within the solution. Therefore, if the conductivity of the solution is high, jet stretching will increase, resulting in smaller fiber diameters. Increasing conductivity can be achieved by adding small amounts of salt or polyelectrolytes [5]. Qin et al. were unable to electrospin polyacrylonitrile (PAN) without the use of salt (lithium chloride). Increasing the salt concentration, increased conductivity and resulted in finer fiber diameters [11]. Arayanarakul et al. were able to electrospin bead-free Polyethylene oxide (PEO) fibers using a sodium chloride concentration above 0.5% (w/v). However, contrary to Qin et al., increasing the salt concentration resulted in an increase in fiber diameters. This was attributed to the delay in the whipping instability caused due to increased conductivity [12].

2.1.2   Process parameters

2.1.2.1 Voltage

There have been contradicting views in the literature concerning the effect of voltage on fiber morphology and diameters. In theory, increasing the voltage increases the charging of the polymeric solution and in turn increases the stretching of the polymeric jet, which reduces fiber diameters [8]. Moreover, increasing voltage also increases the speed of the polymeric jet, shortening the time of travel to the opposite electrode, which in turn can cause wet fiber deposition and formation of beads [13, 14]. Nair et al., however, found that increasing voltage enhanced the morphology of the fibers and reduced beading [15]. These contradicting views are due to the different solvents systems and polymers being used. The effect of voltage is coupled with other solution parameters such as conductivity and surface tension. Cui et al. concluded from statistical analysis using the orthogonal experimental design, that voltage was not as significant compared to the polymer concentration, molecular weight and the solvent system [8].

2.1.2.2 Tip to collector distance

The tip-to-collector distance determines the flight time of the fiber. Larger distance allows for longer flight time and thus more stretching of the fibers and more solvent evaporation; this results in finer, dry fiber formation. However, increasing the distance decreases the electric field gradient, thus a compromise between these two parameters has to be established [5]. Some groups observed bead formation at shorter distances, which was eliminated when distance was increased [16, 17]. Hong et al., on the other hand, was able to control the final morphology by varying the tip-to-collector distance; single layer macroporous films were achieved by reducing the distance, while smooth nanofibers were formed once the distance was increased [18].

2.1.2.3 Feed rate

The feed rate determines the amount of solution being exposed to the electric field at a given time. For every voltage there is a corresponding feed-rate that will allow the formation of a stable Taylor's cone. An interesting study by Ojha et al. showed that using medium molecular weight nylon-6 (50,000 g/mol), beads were formed at low flow rates; increasing the feed rate resulted in smooth fiber formation. However, further increasing the feed rate prohibited electrospinning from taking place. To the contrary, using a high molecular weight nylon-6 (63,000 g/mol) yielded smooth fibers at low feed rates and beaded fibers as the feed rate was increased [17].

2.1.2.4 Orifice diameter

Decreasing needle orifice diameters can reduce the fiber diameters only in some polymers. Katti et al. found that a significant reduction of fiber diameters is observed by using a 20 Gauge needle (inner diameter of 0.584 mm) rather than a16 Gauge needle (inner diameter of 1.194 mm). However, no significant difference in fiber diameters was observed between an 18 Gauge (inner diameter of 0.838 mm) and a 20 Gauge needle [19]. Decreasing the needle diameter beyond a specific diameter may inhibit the extrusion of the solution to the tip [5].

2.1.2.5 Type of collector

The collector in most cases is made of a conductor, in order to remove any accumulated charges on the fibers once deposited on the collector. However, using a non-conductor material as the collector, will result in a charge build up on the surface of the fibers and repulsion among fibers [5]. Therefore, using a non-conductor will produce a lower packing density of fibers compared to a conductor. Different research groups have implemented various collector designs (Figure 3). The fibers form a non-woven, randomly oriented mesh on stationary collectors. However, for some tissue engineering applications, such as nerve regeneration, aligning the nanofibers is essential. The most basic way of acquiring aligned fibers is by using a rotating mandrel [20]. Matthews et al. aligned collagen fibers by rotating the mandrel at 4500 RPM (Figure 3A) [20]. Another method is to use a knife-edge disk as the collector (Figure 3B). This disk will alter the profile of the electrostatic field by focusing the field towards the edge of the disk. The rotation of the disk coupled with the focusing of the electric field allows for excellent fiber alignment [21]. Li et al. proposed a more recent design. The design includes two static collectors with a gap in the middle (Figure 3C). This conformation causes the splitting of the electric field towards the sides of the collectors and thus aligning the fibers across the gap [22].
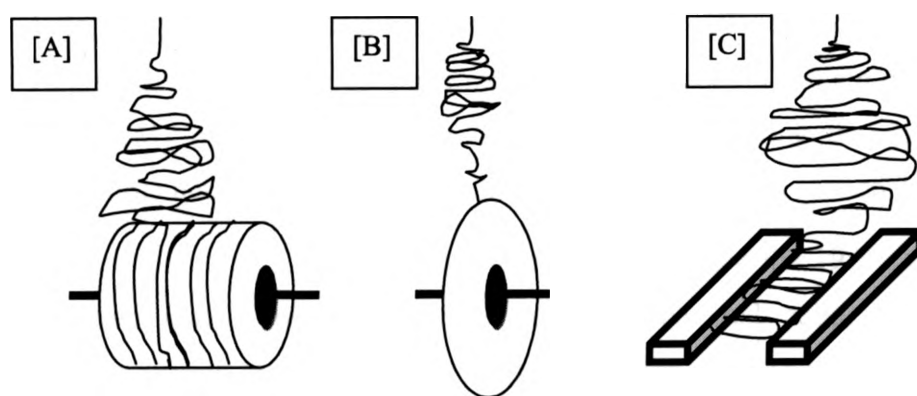
Figure 3. Different types of collectors used to align electrospun fibers: [A] Rotating mandrel, [B] Rotating disk and [C] 'Two-electrodes' setup (Adapted from [20-22])

2.1.3 Electrospinning of natural and synthetic polymers

A wide range of synthetic and natural polymers have been successfully electrospun. Some of these synthetic polymers include: poly(vinyl alcohol) [23, 24],

poly(L-lactic acid) [25, 26], poly(lactide-co-glycolide) [27, 28], poly(urethane) [29], and polycaprolactone [30, 31]. As for natural polymers, both polysaccharides and proteins have been electrospun. Some examples include: gelatin [32, 33], collagen type I [20, 34-37] and type II [38], chitosan [39, 40] and hyaluronic acid [41, 42]. Different groups have also electrospun blends of both natural and synthetic polymers, to achieve characteristics that cannot be achieved by using one of the polymers alone; some of these blends are: gelatin/polycaprolactone [43], chitosan/poly(ethylene oxide) [44], collagen/ poly (ethylene oxide) [45], gelatin/hyaluronic acid [46] and collagen/chitosan [47]. The ability to tailor the chemical and physical structures of these nanofibers allows them to be used in a wide range of applications, especially as scaffolds for tissue engineering. The material this thesis focuses on is electrospinning collagen type I.

2.2 Collagen

Collagen is the most abundant protein in all vertebrates [48, 49]. At present, there are at least 27 different types of collagen that have been discovered [48]. All these collagen types share the same recurring amino acid sequence of (Glycine – X – Y) [50]. They also share the same triple helical structure formed by the intertwining of three peptide chains [48]. They differ however in their macrostructures and their supramolecular assemblies. In addition, each type plays a different role in the tissue they reside in. With all these variations, the definition of a collagen molecule was best stated by Vanderrest et al. as: "A collagen molecule is a structural protein of the extracellular matrix (ECM) which contains one or more domains having the conformation of a collagen triple helix" (a triple helix molecule will be defined in section 2.2.1) [51].

Collagen type I has been studied extensively since the 1950s and was the only type known until 1969 where Miller et al. discovered collagen types II (major collagenous protein in cartilage) and III (accompanies collagen type I in various tissues) [52, 53]. Up till that point, all these collagens were linear fibrils; it was not till 1971 that the study of collagen got more interesting. In 1971, Kefalides et al. discovered collagen type IV in the basement membrane [54] which was structurally different from collagens I, II and III. Type IV collagen forms a meshwork of filaments rather than linear fibrils [51]. Other types of collagens are divided into various categories depending on their structure;

some of them are mentioned here. Linear fibril structures include collagen types I, II, III, V, XI, XXIV and XXVII. Network fibrils include collagen types IV, VI, VIII and X. Fibril-associated collagens with interrupted triple helices (FACITs) are non-fibrillar collagens with the function of binding different molecules in the ECM together, and they include collagen types IX, XII, XIV, XVI, XIX, XX, XXI, XXII [48, 51]. In the following sections, only collagen type I will be discussed, since it is the collagen type used in this thesis.

2.2.1 Molecular structure of collagen type I

The collagen molecule is composed of three polypeptide α chains (2 α_1 and 1 α_2) intertwined to form a triple helix. The α_1 and α_2 chains have similar MWs of ~100,000 and 33% of the amino groups are glycine. However, the chains significantly differ in their amino acid content [55]. Each of these chains forms a left-handed helix and all three form a right-handed super-coil that is stabilized through interchain hydrogen bonds (tertiary structure). Thus, the collagen molecule can be thought of as a coiled-coil triple helical structure [50, 51, 56]. This structure was first proposed by Ramachandran et al. from Madras [57].

The primary structure (i.e. the sequence of amino acids) of each of those chains is responsible for the triple helix formation. Each chain contains 1200 or more residues with glycine repeating every third amino acid [58]. In addition, the sequence glycine-proline-hydroxyproline, occurs in more than 10% of the molecule [50, 56]. This primary structure results in the formation of the left-handed helix (secondary structure) with approximately 3.33 residues per turn, or 10 residues per 3 turns [59]. Every third residue, in individual chains, is located towards the middle of the major triple helix structure, and thus should not contain any side groups, to avoid inter-chain atomic contacts. This explains the appearance of glycine, every third residue [56]. Glycine is the only amino acid that contains hydrogen at both the non-backbone atoms to the α-carbon; this allows for the tight packing of the three peptide chains [60]. The whole collagen molecule is 300 nm long and 1.5 nm wide [61].

The precursor of the collagen molecule, also known as the procollogen molecule, is synthesized in the cell and contains the triple helical structure but with two non-helical

ends attached (the N-terminal and C-terminal). Procollagen is released by the cell into the extracellular space and enzymatically trimmed from the two non-helical ends, forming a collagen molecule that self assembles into fibrils (Quaternary structure). An exception is the formation of small-diameter collagen fibrils, where the N-terminal is not removed during self assembly [50].

2.2.2 Fibrillogenesis

Both X-ray diffraction studies and electron micrographs suggest that collagen fibers are highly organized structures. Collagen fibers exhibit a banding pattern (D-period) that is unique to collagen. The length of this banding is tissue-specific (i.e. 67 nm in rat tail collagen and 64 nm in human dermis) [61]. This banding was first observed in the early 1940s by Wolpers in Germany and Hall et al. in the USA [62]. The first model to explain the banding was suggested by J.W. Smith in 1968 and has been widely accepted [50, 63]. The model stated the formation of microfibrils that involve five collagen molecules that are axially aligned. The lateral and end-to-end aggregation of these microfibrils gives rise to the 'gap' and 'overlap' sections of the collagen fiber [50]. The number of microfibrils assembled, gives rise to different fiber diameters [64].

2.2.3 Role of collagen type I in tissues

The main function of collagen type I is to provide stiffness and mechanical support to the cells in the tissue, especially connective tissue. The three types of cells that produce, absorb, and organize collagen fibers are fibroblasts, osteoblasts and chondrocytes. Fibroblasts are found in many connective tissues, chondrocytes are found in cartilage, and osteoblasts are found in bone. The alignment of collagen fibers can dictate whether the tissue is isotropic or anisotropic. For example, collagen fibers in healthy skin are more randomly oriented compared to scar tissue, which contains collagen fibers oriented parallel to the mechanical loading [65]. In the Submucosa of the small intestine, the collagen fibers run diagonally around the intestine wall, with fibers oriented clockwise and others anticlockwise to achieve a final interwoven architecture of collagen fibers [66]. In aortic heart valves the collagen is aligned circumferentially in the top layer (fibrosa) in order to resist the tension produced by blood during diastole [67]. In

conclusion, collagen is the load-bearing protein and its organization dictates the overall mechanical properties of the tissue.

In addition to dictating mechanical properties of tissue, collagen also contains sites for cell attachment. Culture dishes can be coated with collagen to enhance cell attachment, especially for fibroblasts. Kleinman et al. demonstrated the importance of a glycoprotein called c-CAP (collagen cell attachment protein) to attach trypsinized fibroblasts to collagen. This glycoprotein, usually found on the cell surface, is damaged when the cells are trypsinized (trypsin detaches the cells from the culture plate, in order to be used). Therefore, serum in the growth media acts as an external source of c-CAP, to promote cell attachment to collagen fibers. The sole binding site on the collagen molecule that attaches to c-CAP is found on the $\alpha 1(1)$ chain [68]. In addition, fibronectin (an extracellular matrix glycoprotein) can bind to both collagen and integrins found on the cell surface. Fibronectin can also interface binding between cells and various other extracellular proteins such as fibrin, heparin and gelatin. Interestingly, a research demonstrated the increased affinity of fibronectin to gelatin (denatured collagen) as compared to collagen. It was suggested that fibronectin attaches to the unfolded triple-helices (denatured sections) in collagen fibers, in-vivo, and promotes clearance of these sections from tissues [69].

2.3   Electrospinning collagen type I

2.3.1   Morphology of nanofibers

Matthew et al. reported the first successfully electrospun collagen type I fibers from both calf-skin (CS) and human placenta (HP) [20]. Different concentrations of collagen were dissolved in 1,1,1,3,3,3 hexafluroisopropanol (HFIP), a relatively volatile dipolar aprotic solvent (boiling point of 61 °C). Having a low boiling point is favorable in electrospinning, since it allows the rapid evaporation of the solvent as the jet travels from the tip to the collector, resulting in the deposition of dry fibers. The voltages applied, the distance, and the flow rate were varied to reach an optimal combination of parameters that resulted in bead-less fibers. The optimal results for CS collagen were obtained at an optimal concentration of 0.083 g/ml, a voltage of 25 kV, a distance of 125 mm and a flow rate of 5 ml/hr. These same parameters were used to electrospin HP collagen. The fibers

obtained from CS had average fiber diameters of 100 ± 40 nm and the 67 nm banding pattern native to collagen was observed using transmission electron microscopy (TEM). On the contrary, the fibers obtained from HP were less uniform and resulted in a range of diameters from 100 to 730 nm. The fibers were collected on a rotating mandrel at 4500 RPM, to induce alignment. All electrospun fibers were crosslinked in glutaraldehyde vapor for 24 hours [20]. Subsequent investigation by other research groups adopted glutaraldehyde (GA) vapor crosslinking. Moreover, most groups used HFIP as the solvent.

Groups that electrospun CS collagen type I used similar concentrations to Matthews et al., however different values for the process parameters were used to optimize nanofibers production. Zhong et al. used 0.08 g/ml of CS collagen (from Sigma Aldrich) in HFIP, which is similar to Matthews et al. [37]. However, the voltage used was 15 kV, the distance was 15 cm and the flow rate was 1 ml/hr. The average fiber diameters obtained was 250 nm for the randomly oriented fibers. SEM images show a non-circular cross-section of the fibers as well as bulging that occurs in some areas. Experimental conditions used, and resulting fiber morphologies reported in the literature, are presented in Table 2. It is important to note that none of these groups showed any transmittance electron microscopy (TEM) or atomic force microscopy (AFM) images to confirm the 67 nm banding structure showed by Matthews et al. Moreover, recently Yang et al. confirmed, using circular dichroism (CD) analysis, that the electrospun collagen fibers were partly denatured and this was attributed to the effect of HFIP on destabilizing the triple helix structure. It was claimed that only 45% of the electrospun collagen contained the triple helix structure. In addition, the same group did not observe the 67 nm banding native to collagen in any of the fibers [36].

Table 2. Summary of the electrospinning parameters used by different groups and an SEM of the fiber morphology

Groups	SEM of electrospun CS collagen type I
Matthew et al. [20] [1] *Concentration*: 0.083 g/ml *Voltage*: 25 kV *Distance from collector*: 12.5 cm *Flow rate*: 5 ml/hr *Average fiber diameter*: 100 nm *Collagen purchased from*: Calf skin type I from Sigma Aldrich *Observations*: Fibers have a circular cross section. The 67 nm banding was observed (top right SEM)	
Zhong et al. [37] [2] *Concentration*: 0.08 g/ml *Voltage*: 15 kV *Distance from collector*: 15 cm *Flow rate*: 1 ml/hr *Average fiber diameter*: 250 nm *Collagen purchased from*: Calf skin type I from Sigma Aldrich *Observations*: Fibers don't have a circular cross-section, and bulging occurs when fibers overlap	
Rho et al. [35] [3] *Concentration*: 0.08 g/ml *Voltage*: 15 - 20 kV *Distance from collector*: 8 cm *Flow rate*: 1.2 ml/hr-*Average fiber diameter*: 460 nm *Collagen purchased from*: Calf skin type I from, Regenmed Co. (Seoul,Korea) *Observations*: Fibers don't have a circular cross-section, they are flat	
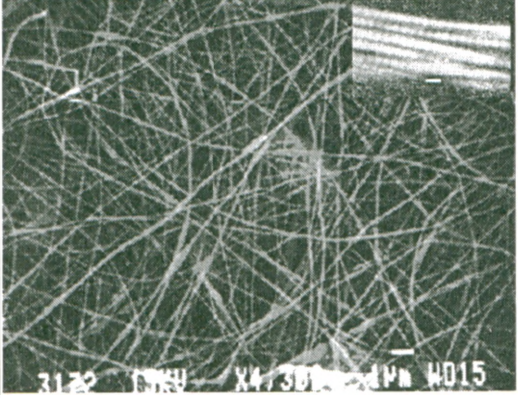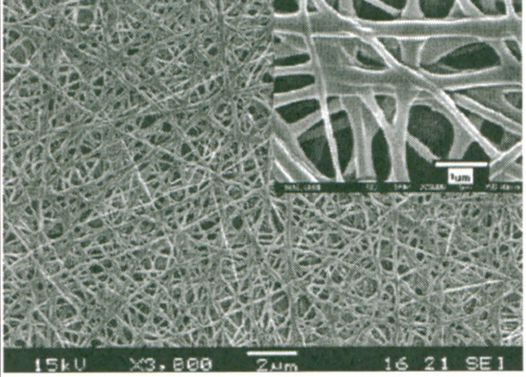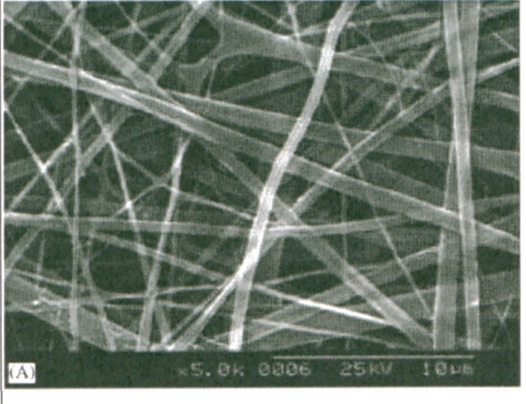
[1] Reproduced with permission from the American Chemical Society

[2] Reproduced with accordance to the "fair dealing" criteria in Canada, provided by John Wiley and Sons, Inc.

[3] Reproduced with permission from Elsevier Limited

Li et al. [70] [4]	
Concentration: 0.083 g/ml **Voltage**: 10 kV **Distance from collector**: 15 cm **Flow rate**: 1ml/hr **Average fiber diameter**: 350 nm **Collagen purchased from**: Calf skin type I from Sigma Aldrich **Observations**: Collagen fibers are straight and AFM confirms that they have a circular cross-section. However, no 67 nm banding has been observed using the AFM	
Yang et al. [36] [5]	
Concentration: 0.08 g/ml **Voltage**: 19 - 21 kV **Distance from collector**: 15 - 20 cm **Flow rate**: 4.8 ml/hr **Average fiber diameter**: 350 nm **Collagen purchased from**: Calf skin type I from Elastin Products Company Inc. **Observations**: Splitting of the fibers can be observed, and fusing occurs at junctions were fibers are overlapping. The authors also report the absence of the 67 nm banding	
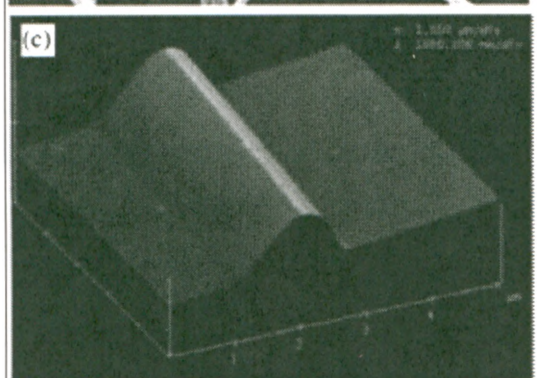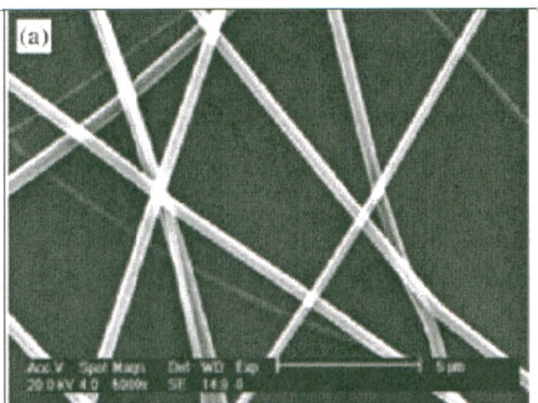
---
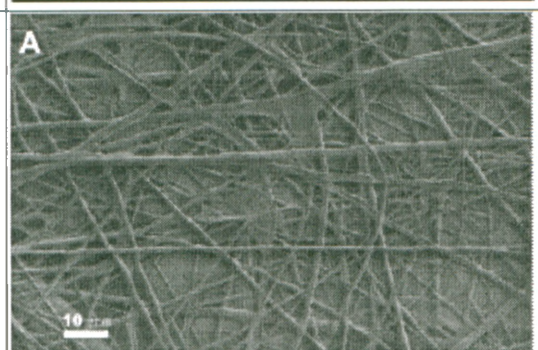
[4] Reproduced with permission from Elsevier Limited

[5] Reproduced with permission from Elsevier Limited

2.3.2 Crosslinking

2.3.2.1 Glutaraldehyde

Currently, most groups use glutaraldehyde (GA) vapor to crosslink their electrospun collagen nanofibers. This is convenient since it does not involve placing the samples in an aqueous environment to perform crosslinking. Exposing electrospun collagen nanofibers to aqueous environments with as low as 5% water cause a rapid fiber swelling and lose of the nanofibrous morphology. Thus, GA vapor was used by most groups to maintain and stabilize the nanofibrous morphology [35]. Rho et al. showed that collagen samples crosslinked using GA vapor for 12 hours, had an 18% reduction in porosity compared to the uncrosslinked sample; this was confirmed from the images presented [35]. Due to the poor final morphology of GA-crosslinked fibers, few groups show post crosslinking images.

Besides the inability to control fiber swelling using GA, another major drawback of GA is its cytotoxicity to cells. Usually after crosslinking with glutaraldehyde the collagenous samples are rinsed in a glycine solution to remove all un-reacted glutaraldehyde. However, even when cross-linked tendon samples were rinsed for up to 6 months, small amounts of glutaraldehyde were released and killed surrounding fibroblasts [71]. Other groups have also confirmed the cytotoxicity of GA [72-74]. This raises the concern over the long-term stability of GA crosslinking. In addition, an ideal scaffold should degrade with time, and if GA is used to crosslink the sample, its release during scaffold degradation can cause significant cell death. Currently, GA is used to crosslink and stabilize bioprostheses that do not contain any cells, and even then, any observed cytotoxicity has been attributed to leaching out of GA into the surrounding environment [75].

2.3.2.2 EDC/NHS

Due to the problems with GA, other crosslinking methods are currently being explored to stabilize electrospun collagen nanofibers. Barnes et al. attempted to crosslink collagen type II electrospun fibers using three different methods: (1) 1-ethyl-3-(3-dimethylaminopropyl) carbodiimide hydrochloride (EDC) in pure ethanol, (2) EDC and N-hydroxysuccinimide (NHS) in pure ethanol and (3) glutaraldehyde solution for

comparing morphology and mechanical properties. Although the authors mentioned the importance of maintaining fiber integrity when soaked in water, the SEM images show significant fiber swelling in solution and the lose of the nanofibrous morphology [76].

Buttafoco et al. were the first group to use EDC/NHS to crosslink electrospun collagen/Polyethylene oxide (PEO) fibers [77]. PEO was used to increase the conductivity of the solution since collagen was being electrospun from a slightly acidic water solution. Sodium chloride was also added to the solution, to produce continuous fibers. Crosslinking was performed by placing the electrospun mats in an EDC/NHS solution of 70% v/v ethanol/water. The authors claimed that no change in morphology was observed after crosslinking. However no SEM images of the final electrospun samples were shown. It is important to mention that, they did not observe the 67 nm banding native to collagen after doing TEM and SEM analysis. This observation is consistent with all the other groups except for Matthews et al. [77].

2.3.2.3 Genipin

Since there still remains a need for a more cell friendly chemical crosslinking agent to stabilize electrospun collagen nanofibers, genipin (a natural crosslinking agent) was investigated in our lab as an alternative to glutaraldehyde. Genipin is a natural crosslinking agent that is derived from geniposide found in the fruits of Gardenia jasminoides Ellis (Figure 4). The geniposide is hydrolyzed with β-glucosidase to produce genipin and when genipin reacts with primary amine groups it produces blue pigments [78]. Recently, genipin has been substituting glutaraldehyde in fixing bioprostheses. Sung et al. in Taiwan have been doing extensive work on the cytotoxicity and biocompatibility of genipin as a crosslinking agent [79-81].
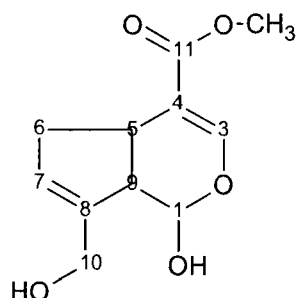
Figure 4. Genipin molecule

Genipin has been found to be ~10,000 times less cytotoxic than GA. In addition, genipin induced ~5000 times greater cell proliferation (3T3 mouse fibroblasts) compared to GA [81]. When a genipin-fixed porcine pericardium was implanted subcutaneously in growing rat models, the inflammatory reaction was less than the GA and epoxy fixed counterparts. It was also found that the calcium levels in the genipin-fixed tissue were minimal throughout the course of the study (12 weeks) but this was not an indication that genipin is fully calcification-proof [82]. Tsai et al. evaluated the geno-toxicity of genipin in-vitro with comparison to GA and found that GA significantly inhibited cell-cycle progression of Chinese hamster ovary cells (CHO-K1), while genipin did not show any delay in the cell cycle. In addition, it was shown that GA can cause a weak clastogenic response (i.e. damage to the chromosomes) while genipin did not cause a clastogenic response in CHO-K1 cells provided its concentration was lower than 50 ppm [83]. Another study by Chang et al. was to evaluate cellular (CP) and acellular bovine pericardia (ACP) fixed with genipin compared to GA. All samples were implanted subcutaneously in a growing rat model. Both CP and ACP fixed with genipin induced a significantly lower inflammatory response compared to their GA counterparts. In addition, the inflammatory reactions for the GA fixed ACP and CP lasted much longer compared to the genipin-fixed counterparts. Moreover, tissue regeneration was faster in the genipin-fixed samples compared to GA [84]. In summary, from all the above studies it can be concluded that genipin is less cytotoxic than GA and hence more biocompatible. Furthermore, genipin led to faster tissue regeneration compared to GA which is very important for tissue engineering applications.

Sung et al. did extensive studies on using genipin to fix collagenous tissues such as the bovine pericardia in comparison with other crosslinking molecules such as GA and

epoxy [79, 80]. In the case of the pericardia fixation, the degree of crosslinking was comparable using all three methods (Genipin, GA and epoxy). The denaturation temperatures of the genipin and GA crosslinked pericardia were significantly higher than those crosslinked with epoxy. The anisotropy of the pericardium was lost when crosslinked with all three methods. However, genipin affected the anisotropy the most, making the mechanical properties (ultimate stress, strain at fracture, modulus of elasticity and toughness) similar in horizontal and vertical samples [79].

Prior to using genipin as a crosslinking agent, researchers in the food industry investigated its use as a food dye. Papers were published that attempted to explain the blue pigment formation when genipin reacted with a primary amine group. Touyama et al. were one of the first groups to study the intermediate brownish-redish pigments that lead to the blue pigment formation [85, 86]. The group emphasized the necessity of oxygen for blue pigment formation. When methylamine (a primary amine) was reacted with genipin, under nitrogen, the reaction mixture turned yellow then brownish-red. The solution turned blue only when oxygen was introduced. In addition, the brownish-red mixture contained pigments that were all intermediates to the blue pigment formation. These pigments were found to be dimers, trimers and tetramers of the molecule 2-methyl-4-carbomethoxy-2-pyrindine, based on spectroscopic analysis [86]. A year later, Touyama et al. published the proposed formation mechanism of those brownish-red pigments [85].

Paik et al. tested the physical stability of the blue pigments formed by reacting glycine, lysine and phenylalanine with genipin. The studies involved testing the stability of the pigments dissolved in buffers with a pH of 5, 7 and 9. Thermal stability was measured with scanning intervals of 30 minutes at temperatures from 60 to 90 °C. Light stability was measured at light intensities of 5000 – 20,000 lux. The optimum pH for blue pigment formation was found to be 7 for all three amino acids. Blue pigments formed by reacting glycine and genipin at 60 °C for 10 hours were more stable in an alkaline pH compared to acidic and neutral conditions. This was due to the formation of more blue pigments from dimer and trimer intermediates. Lysine also formed more blue pigments in an alkaline pH, due to the extra primary amine group. Phenylalanine was also more stable in alkaline conditions. Moreover, under different light intensities, all three amino acids

were stable at 5000 and 10,000 lux. However, at 20,000 lux, blue pigments in alkaline solutions were least stable compared to acidic and neutral environments [87].

Butler et al. demonstrated the mechanism and kinetics of crosslinking biopolymers containing primary amine groups with genipin. Qualitative results showed that: (1) At genipin concentrations below 0.1 mM, there was no significant change in color, while at higher concentrations the solution turned green and then blue, (2) Solutions of acetyl-glucosamine and genipin remained clear, even after days elapsed (i.e. genipin did not react with a secondary amine group), (3) No qualitative difference between mixtures of chitosan and genipin in the dark compared to those exposed to daylight or artificial light, (4) Exposing the mixture to air had a significant influence on the development of the blue color, (5) Using deuterium oxide as a solvent slowed the reaction compared to water and (6) Bovine serum albumin and gelatin solutions with polymers in excess of 10 wt% and genipin concentration of 15 mM and higher were required to form a gel [88].

Ultraviolet-visible spectroscopy, ^{13}C-NMR, protein-transfer reaction-mass spectroscopy, photon correlation spectroscopy and rheology, were all characterization techniques used by Butler et al. to study the genipin crosslinking mechanisms (Figure 5). Two crosslinking reactions that involve different sites on the genipin molecule were proposed. The first reaction involves a nucleophilic attack of the primary amine group on the C3 carbon of genipin to form an aldehyde group. Opening of the ring is then followed by attack of the secondary amine group on the aldehyde group resulting in a tertiary amine group, thus the link is formed between the biopolymers and genipin. This reaction happens immediately after mixing the biopolymers and genipin. The second slower reaction is a S_N2 nucleophilic substitution that involves the replacement of the ester group on genipin by a secondary amide linkage. This was evident due to the release of methanol which was observed only with glucosamine-genipin mixtures and not with acetyl-glucosamines-genipin solutions; this further proves that the primary amine group was the nucleophile in the reaction. This second reaction is slower and requires acid catalysis, which explains the slower reaction in deuterium oxide as compared to water. The author also suggests that more complex reactions take place for the blue pigment formation.

Reaction 1
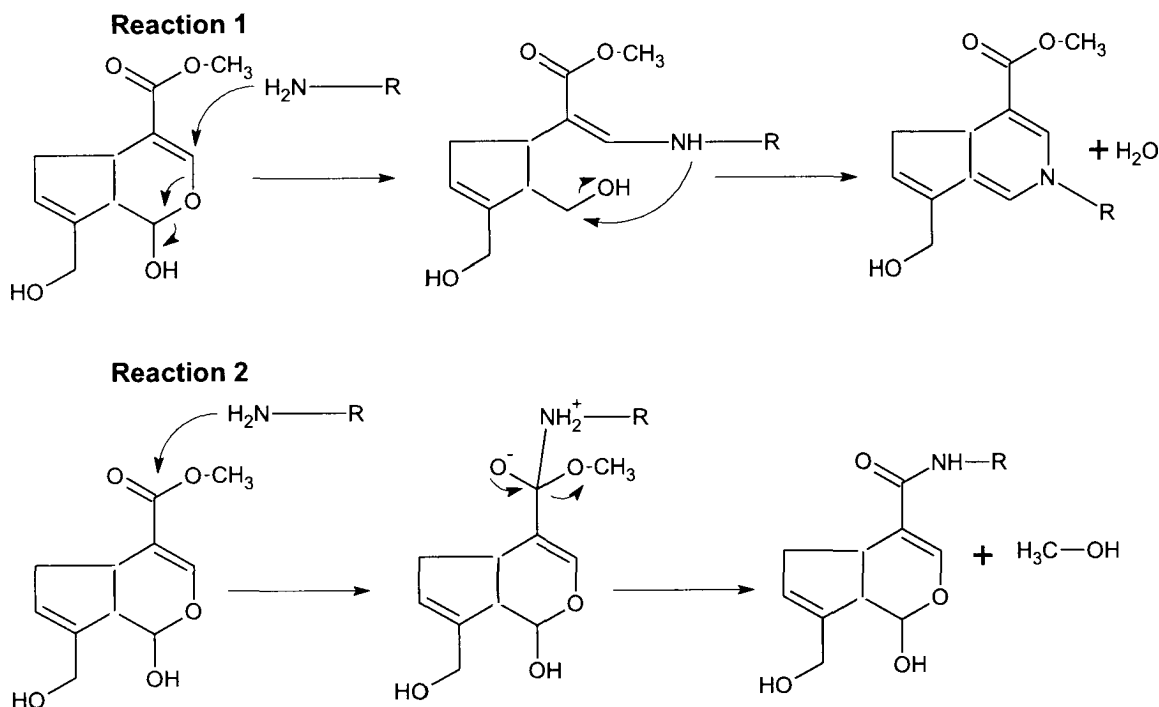
Reaction 2

Figure 5. The two reaction mechanisms between genipin and a primary amine group, proposed by Butler et al. [88]

Mi et al. discovered that genipin can form oligomers after being attacked by a nucleophilic reagent. These oligomers can crosslink chitosan molecules in the form of dimmers, trimers or tetramers. Moreover, this polymerization of genipin does not take place without a nucleophilic reagent [89]. In a different paper, Mi et al. also discovered that genipin self polymerizes at a pH of 13.6 forming a viscous brown solution. The polymerized genipin molecules had molecular weights of 1600 – 20,000 and to consist of 7 – 88 monomers. At a high pH, the nucleophile OH⁻ attacks the genipin molecule and opens the ring to form aldehyde groups. The ring-opened genipin monomers then polymerize via an aldol condensation reaction. At a pH of 1.2, 5, 7.4 and 9 there was no evidence of ring opening polymerization of genipin [90].

Although various groups studied the crosslinking mechanism, the relationship between crosslinking and blue color formation is still controversial. Whether the color change is an indication of crosslinking or just a byproduct of genipin polymerization is a question yet to be answered.

2.4   Cell-substrate interactions

Primary human fibroblasts were the source of cells used in this research. Therefore, a literature review was essential to understand the different cell morphologies that can be acquired based on dimension (2D vs. 3D) and mechanical stress.

Fibroblasts are a type of mesenchymal cells that are migratory and secrete more collagen and fibronectin compared to epithelial cells [91]. Fibroblasts are also capable of secreting growth factors, sensing the mechanical tension in the surrounding tissue and applying forces to other cells and the extracellular matrix [92]. They are considered support cells (provide the structure of tissue) along with chondrocytes (secrete ECM components of cartilage), osteoblasts (secrete ECM components of bone), myofibroblasts (secrete ECM components and have contractile abilities) and adipocytes (lipid-storing cells that have a cushioning and padding function) [93]. All support cells are derived from the mesenchyme, in the mesoderm, during embryological development [91, 93].

For decades, cellular dynamics and processes were studied in a 2D culture environment. It was only recently that cell experiments were carried out in a 3D environment to better mimic the in-vivo conditions [94]. An example of the effect of topography is shown by the difference of mesenchymal cell morphology in 2D versus 3D environments. On a 2D environment (e.g. cover slips), mesenchymal cells form actin aggregated stress fibers, flatten out and lose their migratory abilities. However, in-vivo and on 3D ECM matrices, mesenchymal cells are acquire migratory abilities and possess a bipolar elongated morphology and filopodia (projections that extend from the leading edge of a migrating cell) [91].

In addition to the topography, rigidity of the substrate is also important in guiding cellular morphology and signaling [94-96]. Most of the cell studies in the literature were carried out on 2D, highly rigid, planar surfaces [97], which do not fully mimic the in-vivo conditions [96]. Fibroblasts acquire a flattened, lamellar morphology with actin-aggregated stress fibers when cultured on 2D collagen-coated cover slips [95]. However, upon culturing on 3D collagen matrices that are 'stressed' (i.e. under tension), the cells acquire a bipolar or stellate (i.e. star-like) morphology [95, 98]. Growing fibroblasts in 3D matrices that are not stressed (e.g. floating collagen matrices) yielded   dendritical

extensions in the cells [95, 98, 99], which were identical in morphology to the 'resting' fibroblasts in-vivo [100, 101]. It was also demonstrated that cells on floating 3D collagen matrices had dendritic extensions that were highly dynamic (retracted and protruded) and contained gap junctions that allowed metabolic interactions between cells [95]. Grinnell et al. also studied the effect of platelet–derived growth factor (PDGF), and lysophosphatidic (LPA) on the morphology of fibroblasts in floating collagen matrices [102]. PDGF, which is a pro-migratory protein, caused the dendritic network to protrude, while LPA, which is a pro-contractile phospholipid, caused the retraction of the dendritic network [96]. In addition, the cell density on the floating collagen samples can affect the local and global matrix remodeling processes. Local remodeling was quantified by measuring the movement of collagen-embedded beads towards the cell, while global remodeling was quantified by measuring matrix contraction. Global and local remodeling are also dependent on cell density. A high density of cells (10^6 cells) cause both local and global remodeling to take place, while a low density (10^5 cells) causes local remodeling to take place when PDGF or LPA are introduced [102].

Fibroblasts cultured on 3D stressed collagen matrices undergo proliferation, while cells cultured on floating collagen gels acquire a quiescent phenotype [103]. In addition, it was reported that the only time fibroblasts in-vivo have a spread morphology with focal adhesions and stress fibers, was during fibrotic conditions (e.g. wound repair) [95]. Fibroblasts can 'sense' the tension of the substrate they are on by using their filopodia and can acquire different morphologies and characteristics accordingly [92].

3 Materials and Methods

3.1 Materials

- The following were purchased from Sigma Aldrich, Oakville, ON, Canada:
    - Rat tail collagen type I
    - 1,1,1,3,3,3 Hexafluoroisopropanol ($\geq$ 99%)
    - Glutaraldehyde (25% in water)
    - Anhydrous Isopropanol (99.7%)
    - Stannous Chloride (anhydrous, 99.99%)
    - Sodium acetate trihydrate ($\geq$ 99 %)
    - Ethylene glycol (spectrophotometric grade, $\geq$ 99%)
    - Ninhydrin (97 %)
- Genipin was purchased from Challenge Bio Products Ltd., Yun-Lin Hsien, Taiwan
- Dulbecco's modified essential medium (DMEM) was purchased from Invitrogen Corporation, Burlington, ON, Canada
- Glacial acetic acid was purchased from Caledon Labs, Georgetown, ON, Canada

3.2 Electrospinning

The electrospinning equipment included: a high voltage power supply (Glassman high voltage company), a metal plate collector connected to the high voltage power supply, and a syringe pump (Kd Scientific Model KDS 101) placed on a mechanical jack for position control. A home-built rotating mandrel was used to align fibers (Figure 6). Disposable 1 ml plastic syringes from BD science, and a blunt-ended 18.5-gauge stainless steel needle were used to introduce the collagen solution into the electric field. A metal electrode was attached to the needle to ground it. The electrospinning parameters controlled were: voltage (V), tip to collector distance (D) and the feed rate (Q). The only solution parameter controlled was the collagen concentration. Fibers were electrospun on aluminum foil that was wrapped around the collector plate.
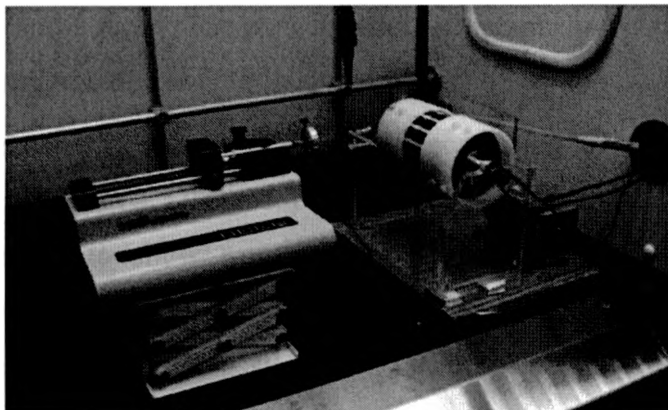
Figure 6. The electrospinning setup with the home-built rotating mandrel

A collagen concentration of 5 wt% dissolved in HFIP, a voltage of 24 – 28 KV, a tip to collector distance of 13 cm, and a feed rate of 0.15 – 0.2 ml/hr yielded collagen nanofibers with no beads. All electrospinning was carried out in a fume hood at room temperature.

3.3   Crosslinking

Two major crosslinking methods were tested in this research: Crosslinking post electrospinning (successful) and crosslinking prior to electrospinning (unsuccessful).

3.3.1   Genipin-crosslinking prior to electrospinning

In this approach genipin was added to the HFIP/collagen solution and mixed for five hours, with the lid open (to expose the solution to oxygen), and electrospun. The solution was mixed for a maximum of five hours, after which gelation occurred and rendered electrospinning impossible. Combinations of experimental parameters such as collagen, genipin, and ethanol concentrations were studied. One of the experimental combinations that yielded collagen/genipin fibers with no beads or genipin crystals included: 3.75 wt% collagen in HFIP, 0.015 M of genipin and 20 v/v% of ethanol (added to reduce viscosity).

3.3.2   Genipin-crosslinking post electrospinning

In this approach, three experimental parameters were varied: (1) the solvent used (isopropanol vs. ethanol), (2) water content in solution (0%, 1%, 3%, and 5%) and (3)

reaction time (1, 3 and 5 days). The concentration of genipin was fixed at 0.03M (~11.3 mg of genipin per mg of collagen) [104].

Electrospun samples were placed in vials containing 20 ml of the crosslinking solution and were placed in a 37°C incubator to speed up the crosslinking reaction. Lids were loosely screwed, to allow exposure to oxygen. After the specified period of crosslinking, all samples were stored in isopropanol or ethanol (depending on the crosslinking solvent used during crosslinking) to maintain sterility until cell seeding was performed.

3.3.3   Glutaraldehyde crosslinking

Crosslinking using glutaraldehyde vapor was achieved by placing the electrospun samples on top of a 25% GA solution for 24 hours. The samples were then washed with PBS and placed in a 0.1M glycine solution overnight, to remove any un-reacted glutaraldehyde. A final washing in PBS was carried out to remove excess glycine.

3.4   Cell seeding experiments

Primary human fibroblasts were acquired from the palmar hand fascia of patients that underwent carpal tunnel release surgery. The primary culture obtained from the clinical specimen were maintained in α-MEM + 10% FBS + antibiotics until use [105]. All fibroblasts used were passaged less than 7 times.

3.4.1   Cell attachment

The growth media in culture plates, containing fibroblasts, was aspirated (sucked out) and the cells were washed with PBS. 3 ml of trypsin was added and the culture plate was placed in an incubator for 5 minutes to detach the cells. 1 ml of growth media (α-MEM supplemented with 10% FBS, streptomycin, and glutamine) was then added to deactivate the trypsin. The solution containing cells was then placed in a centrifuge tube and was centrifuged for 4 minutes. The supernatant was then aspirated, without breaking the pellicle (i.e. cells) and 1 ml of growth media was added. The pellicle was then broken and the solution was pipetted up and down until a uniform solution of cells was formed. A cell count was then performed using a hemocytometer and the solution was diluted to acquire the desired cell concentration.

The crosslinked collagen samples were washed thoroughly with PBS and placed on glass cover slips for 30 minutes. Samples were then placed in a 24-well plate and seeded with 2.5 x 10^4 cells/well for 24 hours.

After 24 hours of cell seeding, the samples were rinsed in PBS by placing them on a shaker for five minutes and were then fixed in paraformaldehyde for 45 mins. They were then washed twice with PBS and the cells were permealized using a PBS + 0.1% TritonX100 solution. Two washes with PBS + Tween were then carried out following a 3% BSA (Bovine Serum Albumin) in PBS + Tween to block unspecific binding sites. Another two washes with PBS+Tween were carried out and the plate was covered in aluminum foil to avoid photo bleaching. 0.5ml of Alexa 488 phalloidin was used (20 minutes on shaker) to stain for the actin cytoskeleton. After two washes with PBS+Tween, 0.5 ml of DAPI stain was used (20 minutes on shaker) to stain the cell nucleus. Finally, two washes with PBS+Tween were carried out and the samples were mounted onto slides. All samples were left to dry overnight before imaging.

For reproducibility, the experiment was repeated three times with different electrospun/crosslinked batches. A preliminary analysis was carried out by doing a cell count on each sample after 24 hours of cell seeding. Five images were taken at 5 different regions (field view of 0.595 mm^2) of each sample (n=3) and the nuclei were counted using Image J (Image processing and analysis in Java – National Institute of Health). This was done to all three runs of each crosslinking condition, for the three different batches (i.e. 45 regions counted per crosslinking condition); the magnification was kept constant for all images.

3.5 Characterization

3.5.1 Scanning electron microscopy (SEM)

A Leo 1530 Scanning Electron Microscope was used to acquire images of both as-spun and crosslinked collagen nanofibers. The accelerating voltage used was 2 kV, which was low enough to avoid the use of conductive coating material on the sample surfaces.

3.5.2 Critical point drying

A critical point drier EMS-850 (Electron Microscopy Science) was used to dry wet samples prior to acquiring SEM images. Samples were dehydrated three times in isopropanol prior to critical point drying. The specimen chamber was filled with liquid carbon dioxide and was then heated beyond the critical point of carbon dioxide at 35°C and 8.6 MPa before depressurizing at a rate of 0.6 MPa/min.

3.5.3 Fourier-transform infrared spectroscopy (FTIR)

Infrared measurements were performed using a Bruker Vector 22 Fourier Transform Infrared (FTIR) spectrometer with an ATR attachment (Pike Technologies Inc., Madison, WI) and a diamond. The spectra were collected in absorption mode, using 64 scans, with a resolution of 4 cm^{-1}.

3.5.4 Fiber diameters

ImageJ was used to measure the fiber diameters. The scale bar (1 μm) on the image was measured in pixels and the fiber diameters were also measured in pixels. The fiber diameters, in nanometers, were calculated as follows: $\dfrac{Diameter_{pixels}}{Scale\ bar_{pixels}} \times 1000$

Four SEM images were acquired for each electrospun sample and twenty-five fibers were randomly picked from each image and measured. Thus, the total fiber diameters measured were 100 for each sample.

3.5.5 Fiber swelling

Two stages of fiber swelling occur during genipin crosslinking. The first stage is the swelling that takes place during crosslinking, and the second stage is further swelling that occurs upon exposure to growth media.

To measure the first stage of swelling (as-spun and after crosslinking): A 100 fiber diameters of as-spun fibers were measured (n=3). The average as-spun fiber diameter was then calculated ($D_{as\text{-}spun}$). The average fiber diameters of crosslinked samples (100 fiber diameters) were also measured ($D_{crosslinked}$), and the swelling was determined using the equation: $\dfrac{D_{crosslinked} - D_{as\text{-}spun}}{D_{as\text{-}spun}} \times 100$.

To measure the second stage of swelling: Each crosslinked electrospun sample was cut in half and one half was placed in anhydrous ethanol/isopropanol (depending on the solvent used during crosslinking), while the other half was placed in DMEM for the required period of time (2,5 and 7 days). Using two halves of the same sample eliminated the effect of minor fiber diameter differences between different electrospun samples, thus producing more accurate results. Also, samples that were in DMEM were rinsed for 2 minutes in distilled water before imaging, to remove any deposited salts on the fibers. Average fiber diameters were then measured after DMEM exposure (D_{final}) and one-way ANOVA using the Tukey test was used to compare the difference between the diameters of crosslinked samples ($D_{crosslinked}$) and after exposure to growth media for 2, 5 and 7 days (D_{final}). If there was a significant difference, the percent swelling was then calculated using the equation: $\dfrac{D_{final} - D_{crosslinked}}{D_{crosslinked}} \times 100$.

3.5.6 Degree of crosslinking

A ninhydrin solution was prepared according to Starcher et al. [106], however the quantities used were different. A 4 N sodium acetate buffer was prepared by dissolving 544 g of sodium acetate trihydrate in 100 ml of glacial acetic acid and 400 ml of distilled water. The solution was left to mix overnight and the final pH was measured to be 5.5. A stannous chloride solution was prepared by adding 100 mg of $SnCl_2$ to 1 ml of ethylene glycol. The resulting solution was cloudy.

The ninhydrin solution was prepared by dissolving 800 mg of ninhydrin in a mixture of 30 ml of ethylene glycol and 10 ml of the 4 N acetate buffer. 1 ml of the stannous chloride suspension was added and the solution was stirred for one hour until the final reagent was pale red. A linear calibration curve was created using different glycine concentrations (Refer to Appendix A).

Crosslinked samples were dried and weighed (W_{sample}) before performing the assay. Samples were then placed in vials containing 2 ml of distilled water mixed with 1 ml of the ninhydrin solution. The vials were placed in an 80 °C water bath for 15 minutes and then left to cool down. The crosslinked samples were removed and a Beckman DU spectrophotometer was used to measure the optical absorbance of the solution at 570 nm, which is the typical absorbance for the purple complex that is formed upon the reaction of ninhydrin with amino acids.

After measuring the absorbance, the calibration curve was used to determine the concentration of free amino acids in solution. The mass of free amino acids (W_{free}) was calculated by multiplying the concentration and the volume (3 ml). The ratio of amino acids released from the collagen sample was calculated ($R = \dfrac{W_{free}}{W_{sample}}$) and the degree of crosslinking for each combination was calculated as follows: $1 - \dfrac{R_{crosslinked}}{R_{as-spun}}$

3.5.7 Fiber stability

The effect of hydrolysis on the crosslinked samples was tested after 1, 3 and 7 days in distilled water. Three samples (n=3) were used for each crosslinking condition (4 crosslinking conditions), at each time point (36 samples in total). All samples were dried in a 37 °C incubator overnight. The dried samples were weighed using an analytical balance. Crosslinked samples were then placed in cuvettes containing 1 ml distilled water for 1, 3 and 7 days in an incubator at 37 °C. After each time point the crosslinked samples were removed from the cuvettes and the solution was stored at 37 °C.

The main objective was to quantify the amount of free amino acids in the distilled water, and calculate the percent weight lost for each sample. A ninhydrin solution

(prepared as previously mentioned in section 3.5.6) was used to detect free amine groups in the distilled water. 0.5 ml of ninhydrin solution was added to the 1 ml solvent in each cuvette. The cuvettes were mixed thoroughly, and placed in an 80 °C water bath for 15 minutes. The solutions were then left to cool for 15 minutes before reading the UV absorption at 570 nm. The absorbance was converted to concentration using the glycine calibration curve. The weight of amino acids in solution was calculated by multiplying the concentration by the volume (1.5 ml). Finally, the percent weight lost was calculated by normalizing the weight of amino acids in solution by the dry weight of the samples, multiplied by a 100.

3.5.8   Fluorescence Microscopy

The fluorescence microscope used was an Olympus IX81. Two filter cubes were used, one for DAPI and the other for ALEXA 488. Exposure time was kept minimal to avoid oversaturation of the samples.

3.5.9   Statistical Analysis

All statistics were performed using OriginPro8 (OriginLab corporation). A one-way ANOVA was used to compare the significance between different groups; unless otherwise mentioned.

4 Results and Discussion

Crosslinking is essential to stabilize electrospun collagen nanofibers in aqueous environments and to enhance their mechanical properties. Using a chemical crosslinking agent with minimum cytotoxicity is desirable and many research groups are probing for alternatives to glutaraldehyde. Genipin has been proven to be ~10,000 times less cytotoxic compared to glutaraldehyde and therefore was investigated as the crosslinking agent in this research, since it is more cell-friendly. The main challenge in this project was to maintain the nanofibrous morphology of the scaffold after crosslinking and also after exposure to an aqueous environment. Losing the nanofibrous morphology after crosslinking or after exposure to an aqueous environment (e.g. cell growth media) renders electrospinning useless. In addition, the ability to control fiber swelling was investigated by using different crosslinking conditions. Controlling the degree of fiber swelling is essential if these fibers were to be used as carriers for drug delivery [107, 108]. Most research groups do not report the fiber morphology in the form of high-resolution images after crosslinking, and none show images after exposure to an aqueous environment. In this research, the nanofibers morphology was studied after crosslinking and after exposure to growth media for up to 7 days. In addition, the swelling and degradation were measured for up to a week in growth media. Cell compatibility was also studied using primary human fibroblasts.

4.1 Optimizing the electrospinning parameters

Different collagen sources, collagen concentrations, and solvent systems were examined until optimum parameters, which resulted in good quality electrospun nanofibers, were acquired. Calf skin collagen type I was the source of collagen used in the literature, and thus was first studied (Table 2). The only solution parameter varied was the collagen concentration. At each concentration, the process parameters (V, Q and D) were varied to optimize fiber diameters and morphology. Initially, optical images were used to examine beadings in the fibers. At 1 and 2 wt% of collagen in HFIP, dripping occurred at the tip of the needle and very few scattered fibers were formed. At 3 wt% (V = 22 KV, Q = 0.05 ml/hr, D = 12 cm), more fibers formed; however beads were still present (Figure 7). Increasing the concentration to 4 wt% yielded smooth fibers with

few beads, while further increasing the concentration to 5 wt% (V = 22 KV, Q = 0.2 ml/hr, D = 13 cm), fully eliminated the formation of beads (Figure 8A).

Rat tail collagen type I was later used instead of calf skin collagen, due to problems with stability of calf skin collagen nanofibers in air. The optimal rat tail collagen concentration was 5 wt% and the optimized electrospinning parameters were: V = 24 - 28 KV, Q = 0.3 - 0.4 ml/hr and D = 13 cm (Figure 8B).

It is important to note that attempts were made to electrospin collagen from other solvents such as acetic acid/water and ethyl acetate/acetic acid/water solutions [109]. However, in all cases electrospinning failed and electrospraying (i.e. formation of droplets in the presence of an electric field) occurred instead.
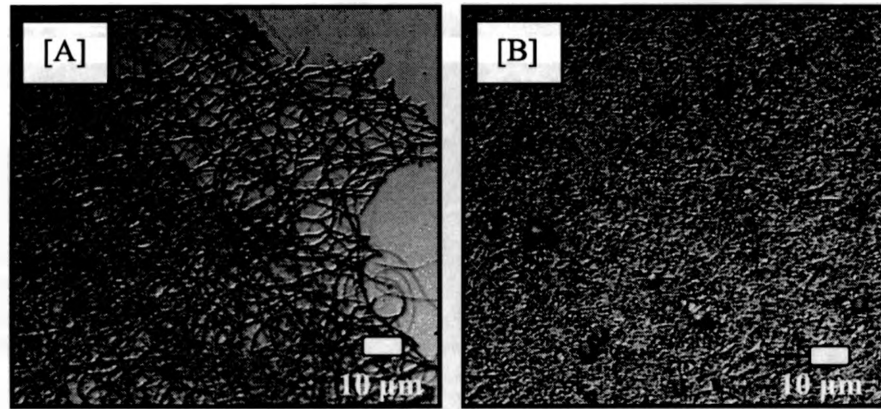
Figure 7. Optical images of electrospun collagen nanofibers using 3 wt% collagen dissolved in HFIP [A]; beads can be observed in more dense areas [B]
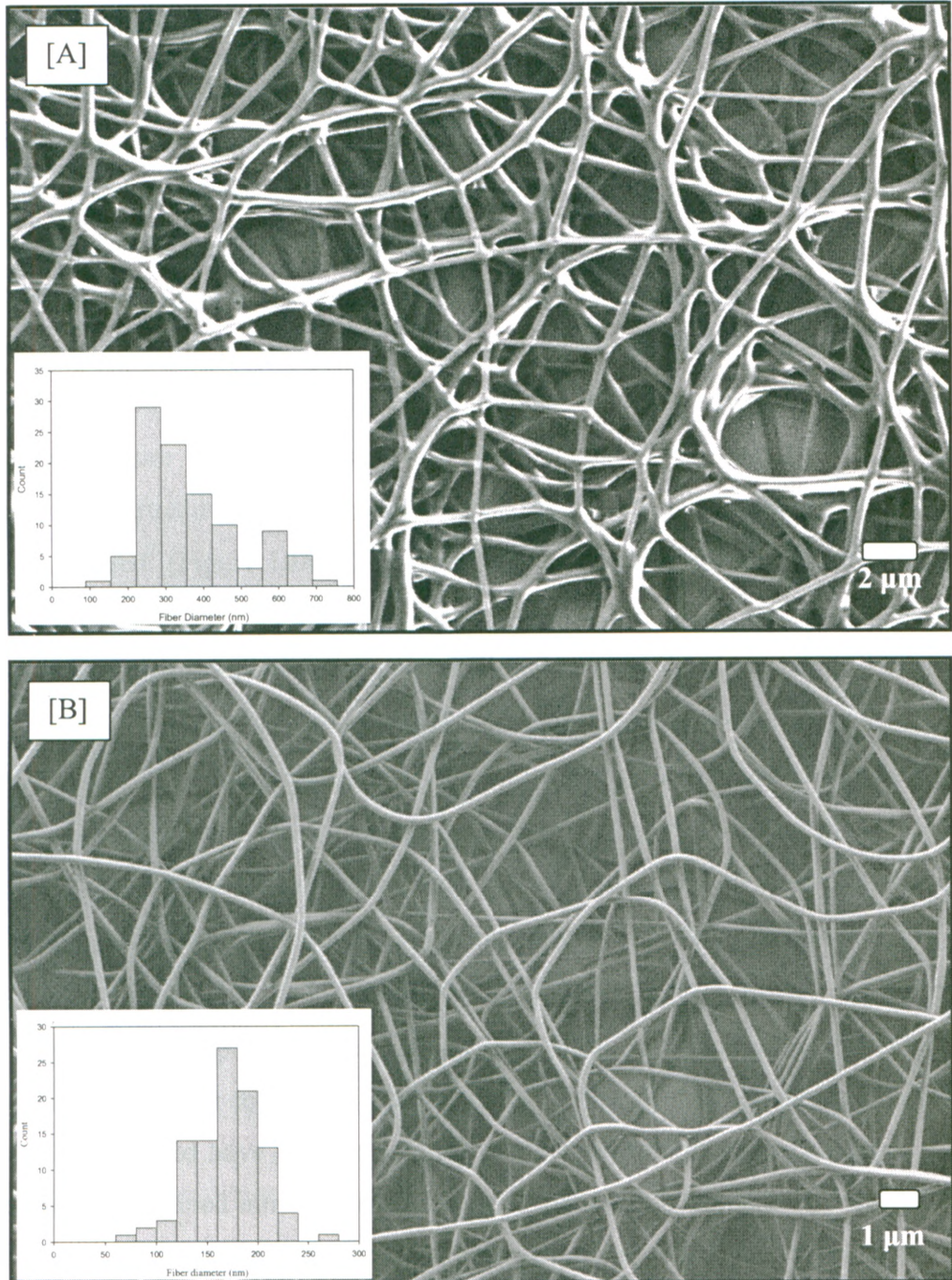
Figure 8. [A] SEM images of electrospun calf skin collagen nanofibers (5 wt% in HFIP) and [B] electrospun rat tail collagen nanofibers (5 wt% in HFIP) - Histograms show the fiber diameter distribution

4.2   Morphology of the as-spun nanofibers

Electrospinning calf skin collagen resulted in fibers with an average diameter of 365 ± 133 nm. The fibers formed a network rather than a true non-woven structure. Overlapping and adjacent fibers fused together at intersecting junctions. This network morphology was thought to be due to the 'wetness' of the fibers (i.e. presence of HFIP in the fibers) when deposited on the collector. In an effort to overcome this problem, the tip to collector distance was increased to 17 cm and air was blown from a nozzle adjacent to the tip of the needle, to enhance solvent evaporation. However, the fiber morphology was unchanged (Figure 9). Also, storing the fibers in the refrigerator (4 °C) in order to preserve their structure prior to imaging caused the fibers to lose their morphology and appear 'annealed' (Figure 10A). The effect of lower temperatures (0°C and -10°C) was also studied by placing the samples in sealed cuvettes, in a water bath overnight, and the fibers also lost their morphology (Figures 10B and 10C).

Rat tail collagen, on the other hand, yielded smooth fibers with an average fiber diameter of 171 ± 34 nm (approximately half the average fiber diameter of calf skin) and the fiber diameters were more consistent compared to calf skin. The fibers were non-woven and no fusing of the fibers took place. Also, there was no change in the morphology after placing samples at low temperatures (4°C to -10°C) overnight (Figure 10D).

There are two possibilities that can explain the calf skin collagen's behavior as compared to the rat tail collagen. First, the purity of the calf skin collagen purchased from Sigma Aldrich could have been of a lower grade compared to rat tail collagen (i.e. calf skin collagen contained other molecules such as glucosaminoglycans or polysaccharides, while rat tail contained less or none), or secondly, there was a difference in the native degree of crosslinking or amino acid composition between the two. Although there is no exact comparison between calf skin and rat tail collagens in the literature, there has been a study on the different physical/chemical properties of collagen type I from various species (Bird feet (BF), bovine skin (BS), frog skin (FS), porcine skin (PS) and shark skin (SS)) [110]. For example, the thermal stability of all collagens was measured using

differential scanning calorimetry, and the collagen with highest thermal transition temperatures was found to be BF, while the least was SS.

    As-spun collagen nanofibers from both sources (calf skin and rat tail) lost their nanofibrous morphology in water or growth media, since the fibers underwent a high degree of swelling and disintegrated to form a film-like structure (Figure 11). Therefore, crosslinking was essential in controlling the fiber swelling and maintaining the nanofibrous structure in aqueous environments. For all the subsequent experiments, rat tail collagen was used.
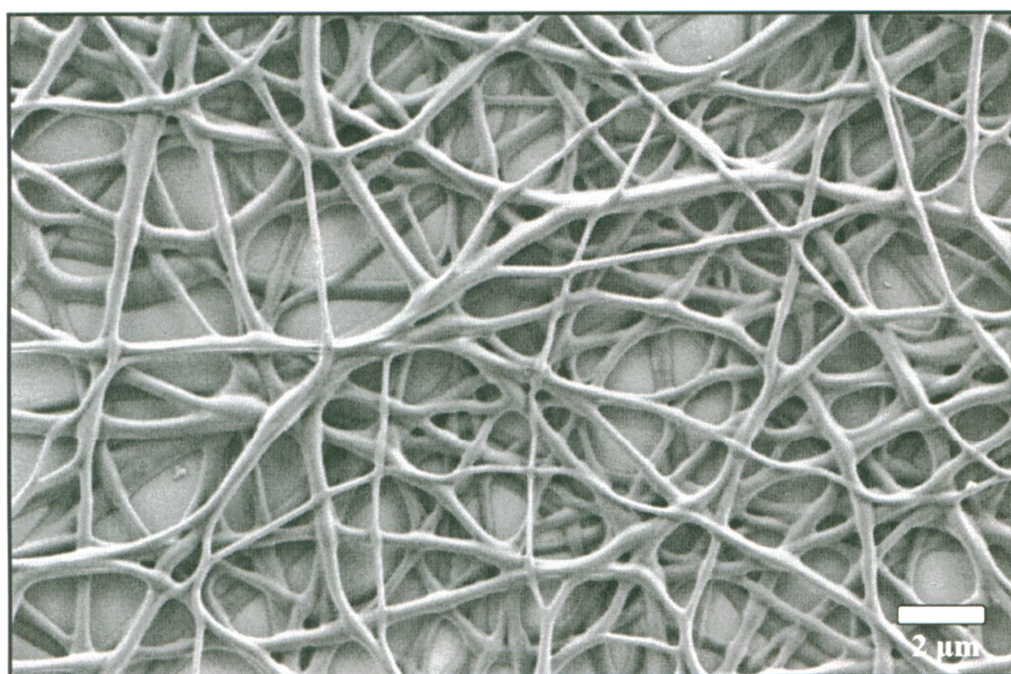
Figure 9. SEM image of electrospun calf skin collagen nanofibers after increasing tip to collector distance to 17 cm and blowing air at the needle tip to try to evaporate the solvent before depositing on collector
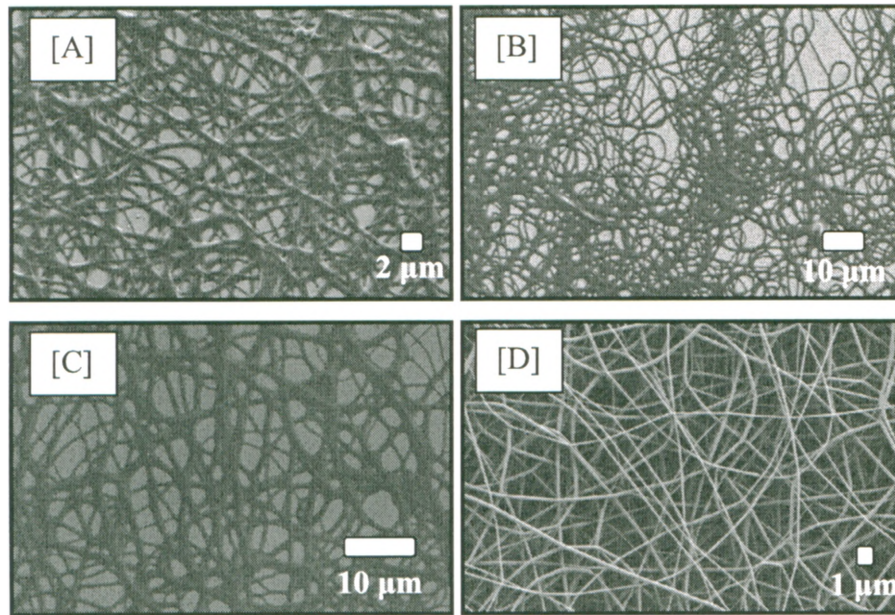
Figure 10. SEM image of electrospun calf skin collagen nanofibers after placing at [A] 4 °C, [B] 0 °C, [C] -10 °C overnight, and rat tail collagen nanofibers [D] at -10 °C overnight
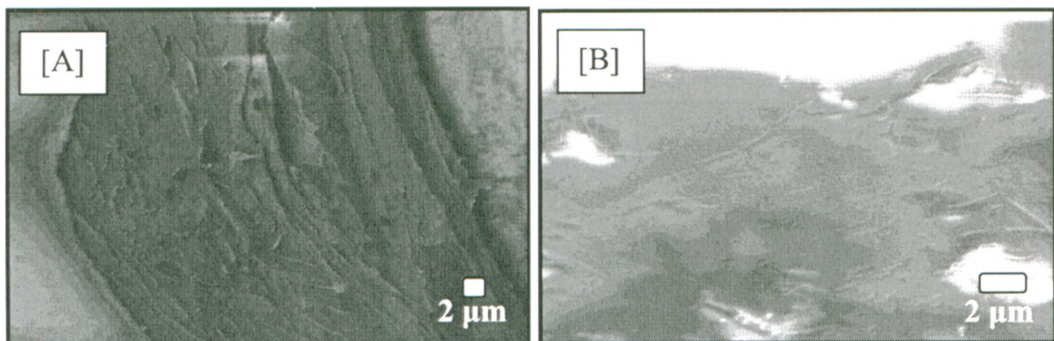
Figure 11. SEM images of [A] rat tail collagen and [B] calf skin collagen after exposure to water for 5 minutes

4.3   Aligning collagen nanofibers

Collagen nanofibers were aligned using two different collector designs: (1) the 'two-electrodes' method, which was introduced by Li et al. [22], and (2) a home-built rotating mandrel. The 'two-electrodes' method with a gap of 1.5 cm produced a higher fiber alignment compared to the rotating mandrel (Figures 12 and 13). However, obtaining a thick mat of aligned fibers was not possible using the two-electrodes method and a rotating mandrel had to be used instead. The degree of alignment using a rotating mandrel was poor at low rotation speeds (4.4 – 13.6 m/s), but was improved by increasing the speed up to 17 m/s.

Controlling fiber alignment is important in designing scaffolds for various tissue engineering applications such as: nerve regeneration and re-creating anisotropic 3D structures similar to heart valves and arteries. Fiber alignment was reported to cause cellular alignment [111-114]. In addition, aligned fibers induced a change in gene expressions as compared to randomly oriented fibers [111].
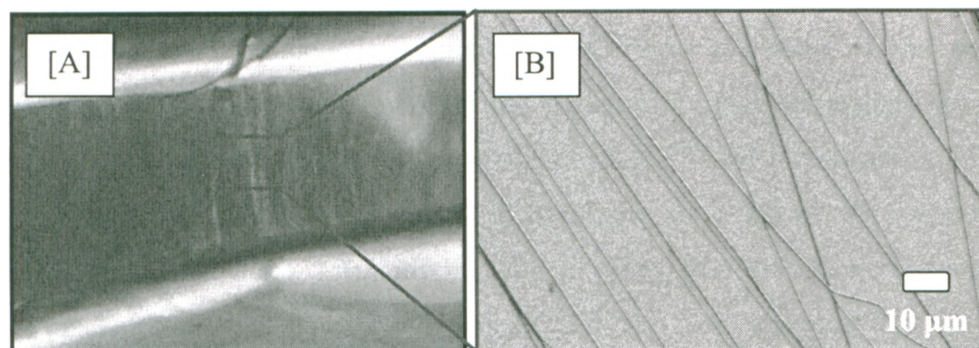
Figure 12. [A] An optical image of the fibers aligning between the two electrodes. [B] SEM image of aligned collagen nanofibers
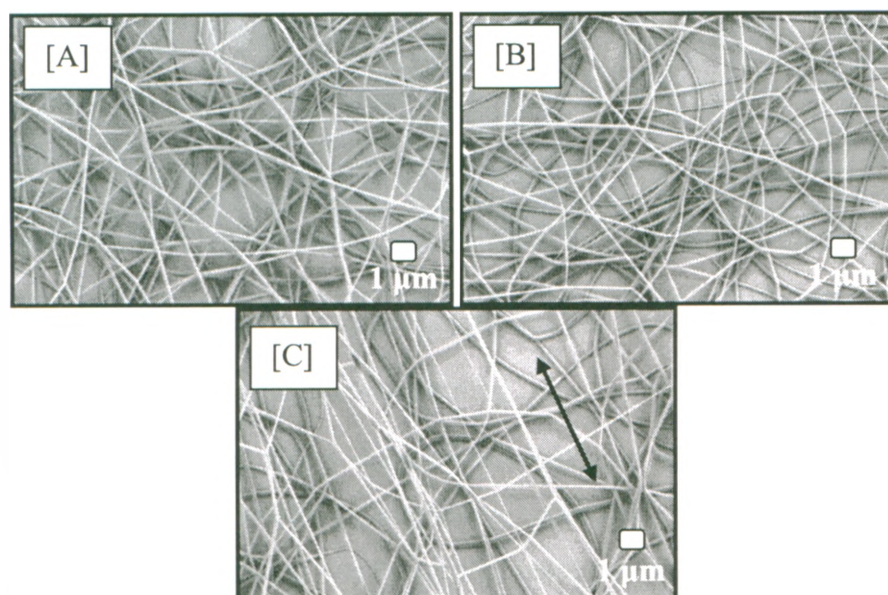
Figure 13. SEMs of collagen nanofibers collected on a rotating mandrel at speeds: [A] 4.4 m/s, [B] 10.27 m/s and [C] 17 m/s (arrow indicates direction of alignment)

4.4   Morphology of crosslinked collagen nanofibers

4.4.1   Fibers crosslinked prior to electrospinning

In this approach, genipin was mixed with the collagen and HFIP solution for a specific period of time, and then electrospun. The experimental parameters investigated in this approach were: collagen concentration, genipin concentration, percent water added, percent ethanol added, and mixing time. However, none of the parameter combinations were successful in maintaining the nanofibrous morphology in aqueous environments. In this section, the results obtained using 3.75 wt% collagen in HFIP with 0.015M genipin and 20 v/v% of ethanol after mixing for 5 hours are presented. The solution turned pale green after mixing for 5 hours and fibers were successfully electrospun. The average fiber diameter was 287 ± 59 nm (~69% greater than the average diameter of as-spun collagen nanofibers). However, fibers lost their morphology after exposure to water for 5 minutes (Figure 14).
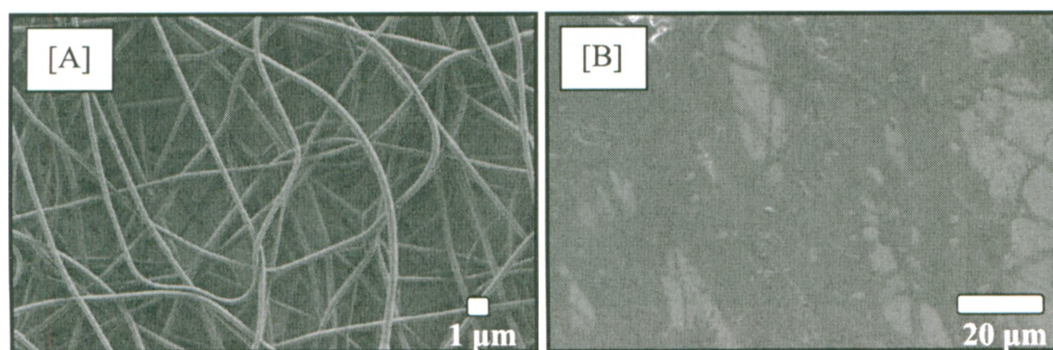
Figure 14. [A] SEM images of electrospun collagen + genipin nanofibers (3.75 wt% collagen + 0.015M genipin, mixed for 5 hours) and [B] after placing in water for 5 minutes

4.4.2   Fibers crosslinked post electrospinning

In this approach the fibers were crosslinked post electrospinning. Since water caused significant fiber swelling, alternative solvents, that maintained the fiber morphology during crosslinking, were required. Isopropanol and ethanol were shown to maintain the fiber morphology, and thus were used as crosslinking solvents. However, a range of genipin concentrations (0.03 – 0.1 M) in absolute ethanol or isopropanol failed to maintain the morphology and overall architecture of the fibers after exposure to water, even after crosslinking for 5 days (Figure 15). It is interesting to note that absolute

isopropanol better maintained the fiber morphology compared to ethanol, and this could be attributed to the higher hydrophobicity of isopropanol as compared to ethanol.

However, with the addition of water it was observed that there were certain alcohol/water concentration combinations that maintained the fiber morphologies. As a result, a systematic study was carried out to determine the effect of changing crosslinking solution composition on collagen fiber stability in an aqueous environment.
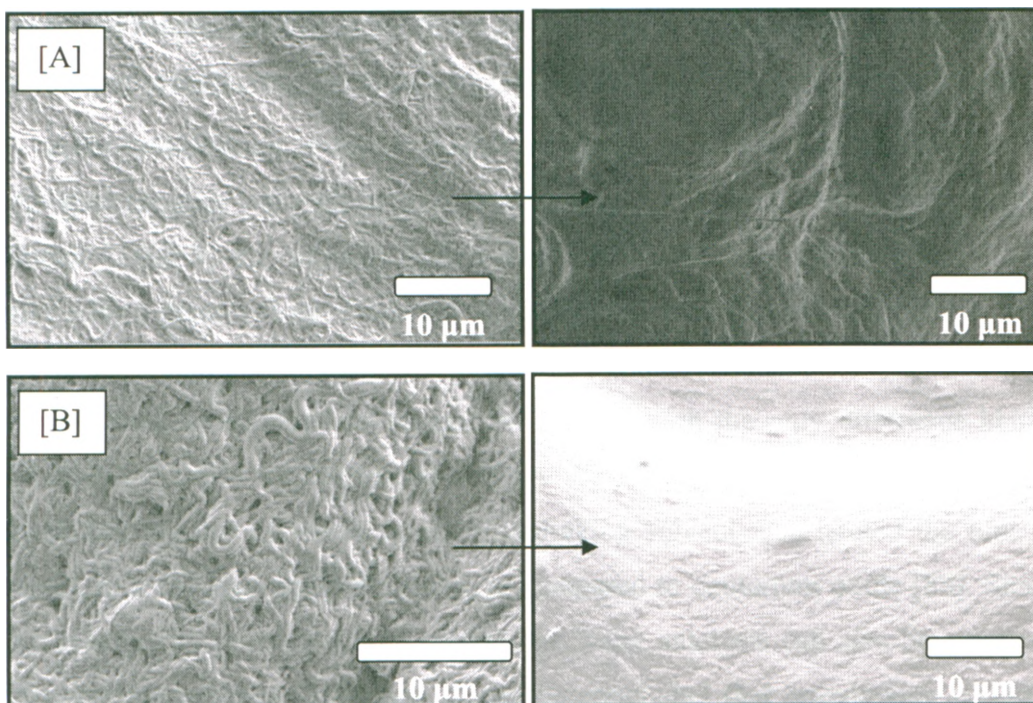
Figure 15. SEM images of collagen nanofibers crosslinked for 5 days in [A] absolute ethanol and [B] absolute isopropanol using a genipin concentration of 0.03M, and after exposure to water for 5 minutes

4.4.2.1 Optimizing crosslinking conditions

In order to determine the optimal conditions for crosslinking, three experimental parameters were studied: crosslinking solvent (ethanol vs. isopropanol), water content added (0, 1, 3 and 5 v/v %) and crosslinking time (1, 3 and 5 days). The optimal combinations were selected depending on the stability of the fibers after exposure to both water and Dulbecco's Modified Eagle's Media (DMEM). Table 3 shows the four combinations that resulted in stable fibers morphology in water for up to 5 minutes. Table 4 lists the four crosslinking combinations with an assigned number to each combination.

After crosslinking, a colour change took place in all crosslinked samples (Figure 16). As-spun samples were white prior to crosslinking. However, upon crosslinking using conditions 1 and 3, the samples turned deep blue, while conditions 2 and 4 yielded samples with a green colour. During crosslinking, all samples were exposed to air, thus the colour difference can be attributed to the water content and alcohol system. Samples 2 and 3 were both crosslinked in ethanol for 5 days, with the only difference being the water content, 3 v/v% for the former and 5 v/v% for the latter. In the literature, it was observed that the use of water, as the crosslinking solvent, accelerated the blue color formation, in a chitosan-genipin system, as compared to deuterium oxide [88]. Since the genipin reacts with primary amine groups, the water catalysis can also be assumed for collagen-genipin systems. Therefore, it can be concluded that crosslinking condition 3 yielded a deep blue colour faster, since more water was available as compared to condition 2. However, condition 4 contained the same amount of water (5 v/v%) as condition 3 and the same reaction time (5 days), but a green colour was produced. This suggested that isopropanol slowed down the action of water since it is more hydrophobic as compared to ethanol. It is also important to mention that samples crosslinked using conditions 2 and 4 eventually turned deep blue upon exposure to water or growth media.

Although there have been several studies on the mechanisms of the crosslinking reaction, its relationship to the blue color formation is still controversial. Butler et al. proposed the two reactions that take place during crosslinking, and does not consider the genipin polymerization reactions, thus, attributes the blue colour formation to 'other complex reactions' [88]. Mi et al. however, demonstrated the ability of genipin to self polymerize after a nucleophilic attack, to form dimmers, trimers and tetramers [89]. The

proposed explanation of colour change as it relates to degree of crosslinking will be further explained in section 4.4.2.3.

Table 3. The four crosslinking combinations that yielded intact fibers with minimal swelling after exposure to water for 5 minutes (✓ - maintained nanofibrous morphology, X – lost nanofibrous morphology due to excessive swelling)

	Ethanol				Isopropanol			
	Water content (v/v %)				Water content (v/v %)			
Crosslinking time (days)	0	1	3	5	0	1	3	5
1	X	X	X	X	X	X	X	X
3	X	X	X	✓	X	X	X	X
5	X	X	✓	✓	X	X	X	✓

Table 4. The four crosslinking conditions studied

Crosslinking condition	Solvent	Water content (v/v%)	Crosslinking time (days)
1	Ethanol	5	3
2	Ethanol	3	5
3	Ethanol	5	5
4	Isopropanol	5	5

Figure 16. [A] As-spun, un-crosslinked, collagen sample and [B] samples crosslinking using the four conditions

4.4.2.2 Fiber swelling

Two stages of swelling were studied: swelling that occurred due to crosslinking and swelling that took place after exposing the fibers to DMEM. The first stage of swelling could be observed by comparing the as-spun fibers (Figure 8B) and the crosslinked fibers (Figure 17, first column of SEM images). Samples crosslinked using conditions 1 and 3 had the highest degree of swelling after crosslinking (196±8 % and 180±7 % respectively), while conditions 2 and 4 had the least swelling (55±5 % and 56±4 % respectively). The effect of water content on the crosslinked fiber morphology is evident. Fibers crosslinked using conditions 1 and 3 (crosslinking solutions containing 5 v/v% water) had higher fiber swelling after crosslinking compared to condition 2 (crosslinking solution containing 3 v/v% water). Condition 4 (crosslinking solution containing 5 v/v% water) yielded lower swelling compared to condition 3, due to higher hydrophobicity of isopropanol compared to ethanol (Figure 18). Also, increasing the time of crosslinking (condition 1 vs. 3) did not cause any significant change in fiber diameters after crosslinking ($P > 0.05$). This illustrates that the water content has a more significant effect on fiber morphology compared to crosslinking time.

Fibers crosslinked using condition 1 did not undergo any significant swelling for up to 7 days in DMEM (Figure 19). Fibers crosslinked using condition 2 underwent 18 ± 3% swelling after 2 days in DMEM, which increased to 24 ± 3% after 5 days and did not undergo any further increase after 7 days. Conditions 3 and 4 yielded fibers that continued to swell for up to 7 days. Fibers crosslinked using condition 3 swelled 5 ± 3%, 10 ± 3% and 23 ± 4% after 2, 5 and 7 days, while for condition 4, the fibers swelled 37 ± 3%, 54 ± 4%, 59 ± 4% respectively (Figure 19). The increase in swelling with time (condition 3 vs. 1) can be attributed to the oligomerisation of genipin with time, thus increasing porosity of the fibers and allowing more swelling to take place [89, 115]. Crosslinking condition 4 yielded fibers with the highest degree of swelling after exposure to DMEM, and this could be attributed to the hydrophobic effect of isopropanol (compared to ethanol), which slowed down the rate of reaction between the genipin molecules and primary amine groups (Refer to section 4.6). These results illustrate the

control of degrees of swelling, in DMEM, that are achievable by a judicious choice of crosslinking condition.

This ability to control swelling of the collagen nanofibers has important implications in tissue engineering. The degree and rate of swelling of these fibers are associated with their strength and rate of degradation. In a tissue engineering environment, the decrease in strength and the rate of degradation of the collagen scaffold has to be designed such that they are comparable to or smaller than the rate of deposition and organization of the extracellular matrix being deposited by the cells, to ensure geometric and structural integrity. Since the rate of extracellular matrix production and organization is cell-type dependent, it is important that the rate of degradation of the scaffold material be properly designed. It is now possible for such control on collagen nanofibrous scaffolds by controlling the genipin crosslinking conditions.
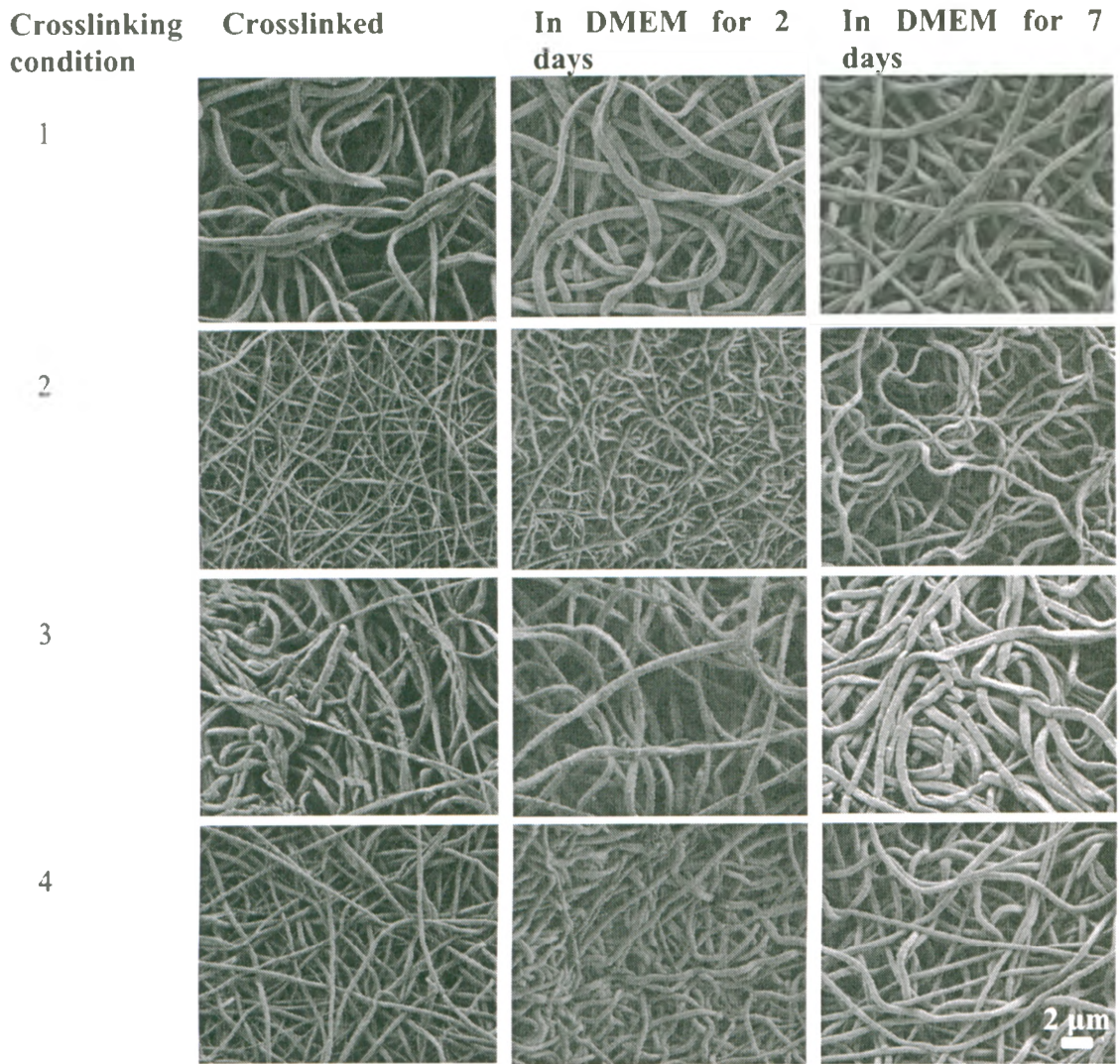
Figure 17. SEM images of the collagen nanofibers after crosslinking, using the 4 conditions, and after placing in DMEM for 2 and 7 days at 37 °C (all the above samples were dried using critical point drying, prior to imaging, to prevent surface tension from altering the 3D structure)
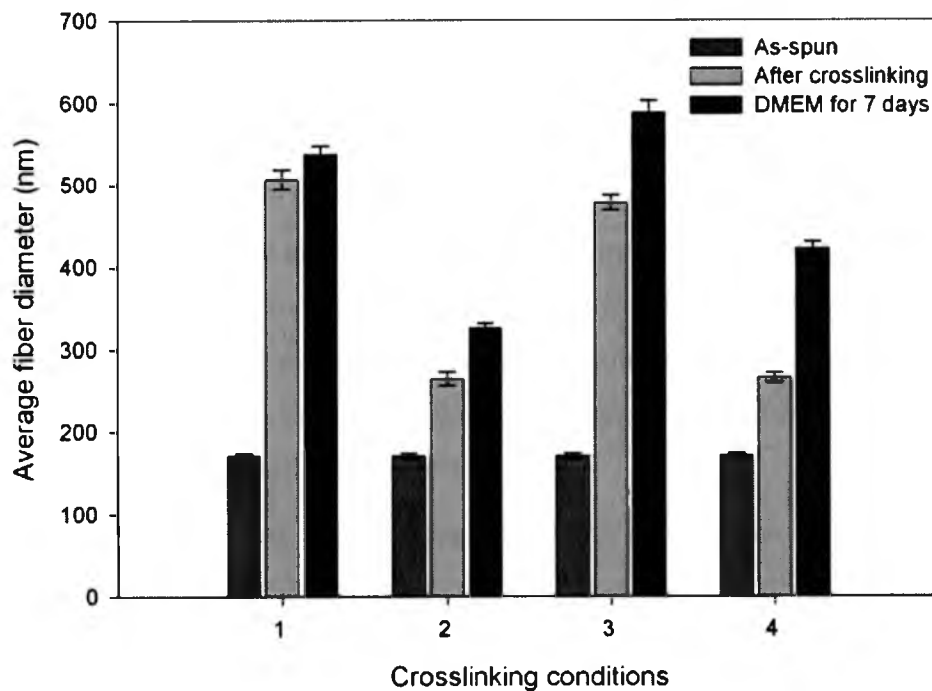
Figure 18. The average fiber diameters with error bars of as-spun fibers, crosslinked, and immersed in DMEM for 7 days for the 4 crosslinking conditions (n = 100)
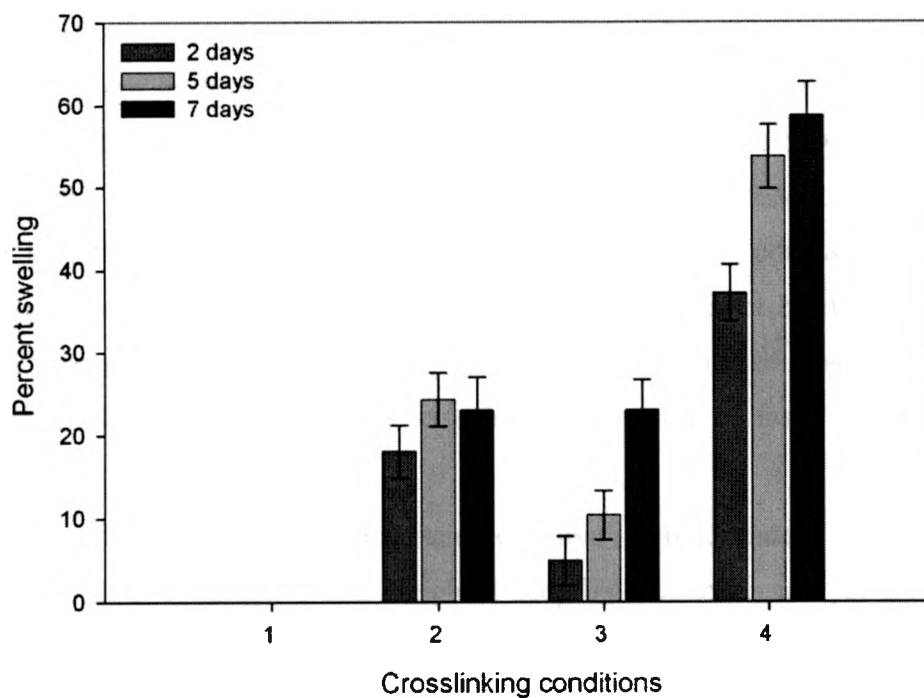
Figure 19. Percent fiber swelling with standard error bars of the samples crosslinked using the four conditions after exposure to DMEM for 2, 5 and 7 days (n = 100)

4.4.2.3 Degree of crosslinking

The ninhydrin assay has been utilized by various groups to quantify the degree of crosslinking of tissue [79, 106, 116]. However, the assay does not provide any information on the density or nature of crosslinking. Two genipin molecules that react with only one primary amine group each, but do not crosslink with another, will give the same result as a genipin molecule crosslinking two primary amine groups [117]. However, if we assume that most of the reactions result in crosslinking, as have shown previously [79, 106, 116], this assay provides a good indication of the degree of crosslinking of electrospun collagen nanofibers.

It can be seen that all crosslinking conditions are effective to varying degrees (Figure 20). Samples crosslinked using condition 3 had less free primary amine groups compared to condition 1 (i.e. higher degree of crosslinking). Condition 2 yielded the highest degree of crosslinking. It is hypothesized that due to the lower water content used in condition 2 (3 v/v%) compared to conditions 1 and 3 (5 v/v %), less fiber swelling took place during crosslinking and thus most of the crosslinking took place on the surface of the fibers. This increased crosslinking density at the surface, hindered the exposure of free amine groups in the core of the fibers to the ninhydrin molecules, and thus resulted in an assay that gives higher degree of crosslinking. This collaborates well with the lower degree of fiber swelling using condition 2, post exposure to DMEM, due to the inability of water to infiltrate into the fibers. Crosslinking condition 4 was comparable to condition 3, although the differences in the nature of crosslinking cannot be determined by the ninhydrin assay. GA-crosslinked samples yielded a high degree of crosslinking within 1 day, which illustrates that the GA crosslinking reaction is faster than its genipin counterpart

It can also be observed that sample colour is independent of the degree of crosslinking. Both condition 1 and 3 yielded deep blue samples, and yet the degrees of crosslinking are significantly different. Also conditions 2 and 3 were crosslinked for five days, having comparable degrees of crosslinking and yet they differ in their colour. Therefore, it can be interpreted that water content and oxygen were responsible for the colour change. An attempt to understand the colour change can be made using the crosslinking reactions found in the literature. From section 4.4.2.1, it was shown that

water is essential in accelerating the blue colour formation and also water is needed to catalyze the nucleophilic substitution that takes place at the ester group on the genipin molecule [88, 89]. In addition, the polymerization of genipin requires an initial nucleophilic attack on the genipin molecule [89]. Therefore, it is suggested that increased water content resulted in an increase in the self polymerization of genipin and the aggregation of aromatic groups with conjugated double bonds gave the samples the deep blue colour. Oligomer link molecules derived from the self-polymerization of genipin can be involved in the collagen crosslinking reaction along with or instead of single molecule genipin crosslinking (Figure 21). This reduction can be observed by comparing samples crosslinked using conditions 2 and 3.
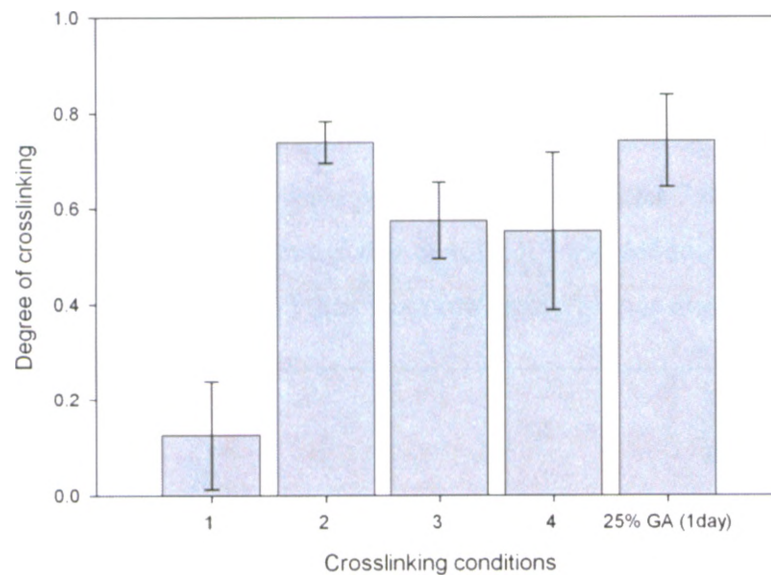
Figure 20. Degree of crosslinking using the 4 conditions and 25% Glutaraldehyde vapor was included for comparison (n=3)

G - Genipin
Collagen
Genipin-Genipin bond
Genipin-Primary amine bond
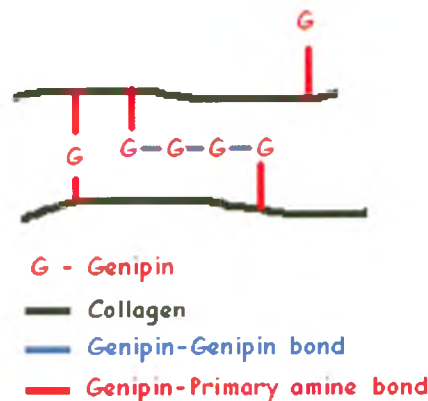
Figure 21. A schematic illustrating the different genipin-collagen crosslinking methods

4.5   Fiber stability

The stability of the crosslinked fibers was tested in distilled water for up to 7 days. A ninhydrin assay was used to determine the amount of free amine groups released in solution. Qualitatively, there were no apparent changes in colour, after the ninhydrin reaction, for all samples. Figure 22 shows the percent weight loss as determined by the ninhydrin assay, in distilled water for all four crosslinking conditions, after 1,3 and 7 days. For all samples, the maximum percent weight loss was 0.3 ± 0.16 % for crosslinking condition 4, after 7 days in distilled water. Crosslinking conditions 1 and 2 had weights loss below 0.1 % after 7 days, while crosslinking condition 3 had a maximum of 0.16 ± 0.02 % after 7 days. These results indicate that the fibers are very stable in distilled water for up to 7 days. These results also correspond well with the swelling data, with crosslinking condition 4 having the most swelling after 7 days and also the highest percent weight lost after 7 days. Also, crosslinking condition 1, which gave the least swelling, also had the least percent weight loss after 7 days, as compared to condition 3. This supports the hypothesis that condition 3 yielded more porous fibers due to the oligomerisation of genipin, and thus the more amine groups dissolving in water.
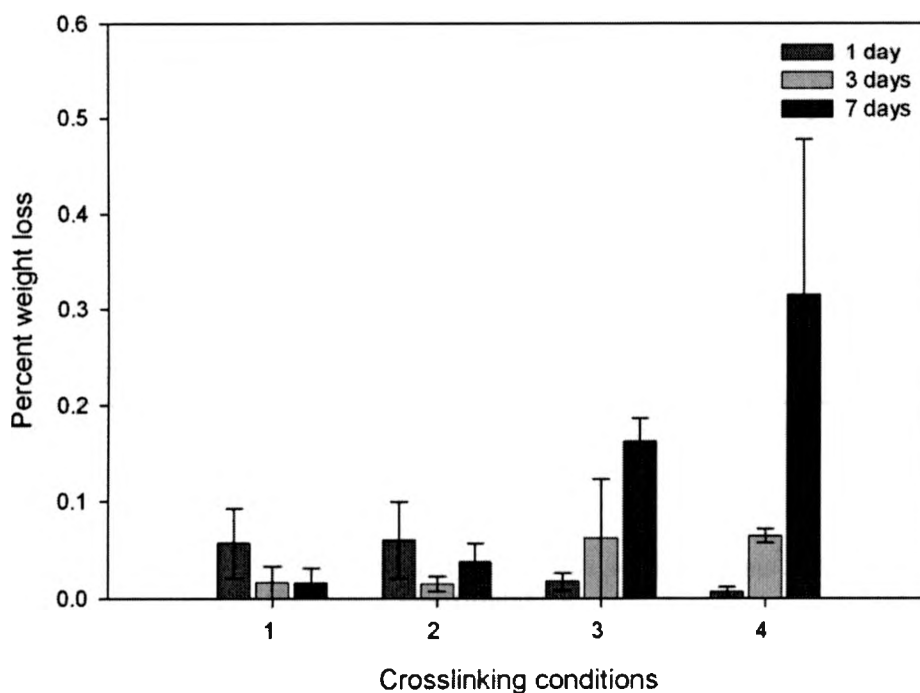
Figure 22. Percent weight loss and standard errors of crosslinked samples, calculated using the ninhydrin assay, after placing in distilled water for 1, 3 and 7 days (n=3)

4.6   Characterization using Fourier Transform Infrared Spectroscopy (FTIR) analysis

FTIR spectra of as-purchased rat tail collagen and the as-spun are shown in Figure 23. It can be shown from the FTIR spectra that all the functional groups are retained after electrospinning, and no traces of HFIP were found. The spectra of the as-purchased and as-spun samples are similar to collagen type I FTIR spectra found in the literature [118, 119]. Absorptions at 1030 and 1082 cm^{-1} are attributed to C-O stretching of alcohol groups, which are present mainly in hydroxyprolines. Absorptions bands at 1201, 1220, 1232, 1282, 1348, 1378 and 1454 cm^{-1} are attributed to the C-H wagging and C-N stretching of collagen. Finally, the absorptions at 1635 and 1554 cm^{-1} are attributed to the Amide I (C=O stretching) and Amide II (N-H bending) respectively. The broad absorption at 3310 is attributed to the O-H stretching in carboxylic acids [120].
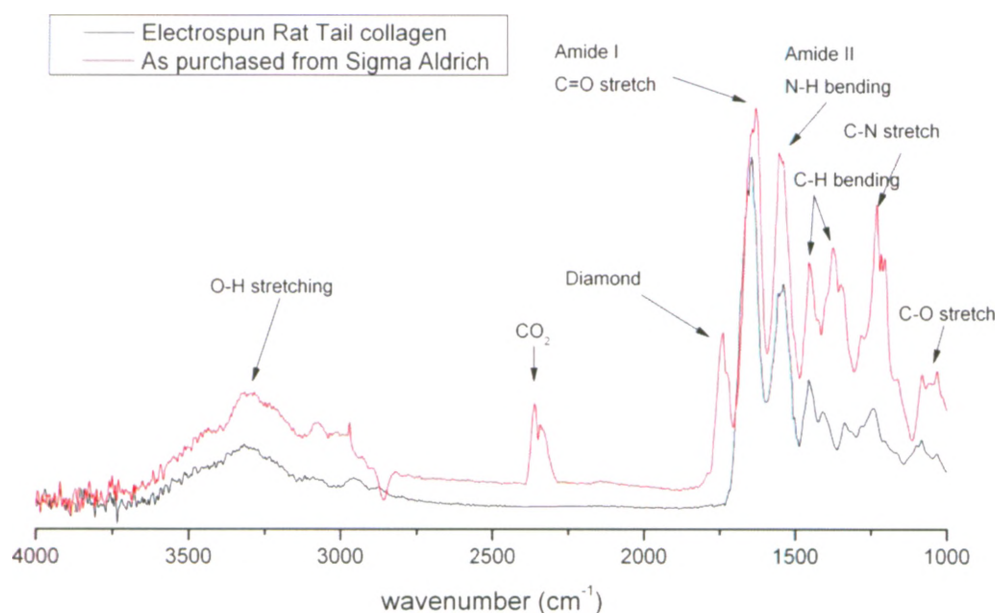
Figure 23. FTIR spectra of as-purchased rat tail collagen from Sigma Aldrich and after electrospinning

The FTIR spectrum of genipin is presented in Figure 24 and it was similar to that found in the literature [89, 121]. Absorptions at 988 and 1084 cm^{-1} are attributed to the ring C-H out-of-plane bending and ring C-H in-plane bending respectively. The absorption at 1084 cm^{-1} may also include the C-O stretch of the primary alcohol. Absorptions at 1299 and 1440 cm^{-1} are attributed to the C-O-C asymmetric stretch and the CH_3 bend of the methyl ester respectively [121]. The absorptions at 1617 and 1680 cm^{-1} are attributed to the ring C=C stretch and C=O from the ester group.
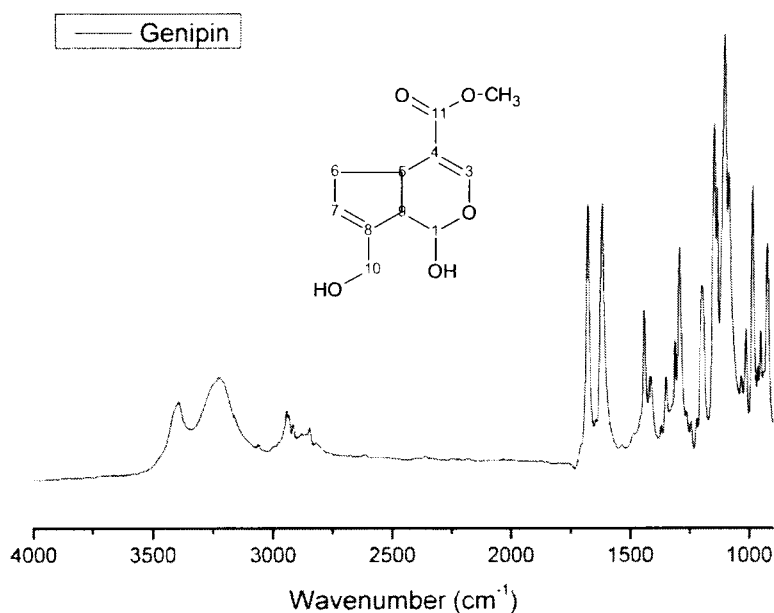
Figure 24. FTIR spectrum of genipin powder

Figure 25 shows the FTIR spectra of the as-spun collagen nanofibers as well as the fibers crosslinked using the four conditions. An expanded view of 1000 – 1600 cm^{-1} is shown in Figure 26. The reaction between primary amine groups, found in the as-spun collagen fibers, and genipin is evident from the disappearance of a peak (1133 cm^{-1}) from the as-spun collagen spectrum upon crosslinking. A weak peak at the absorption 1133 cm^{-1} is attributed to the C-N stretching vibration of a primary aliphatic amine with the structure (-CH-NH$_2$), which is available in lysine and arginine. This peak disappears in all the crosslinked samples.

As previously mentioned, a tertiary amine group is formed after the genipin reaction with primary amine groups and has a strong stretching vibration in the range $1380 - 1330$ cm^{-1} [120]. However, no strong peaks were observed in that range in any of the genipin-crosslinked samples. Mi et al. demonstrated that the C-N stretching of the aromatic tertiary amine group was visible in the range $1300 - 1500$ cm^{-1} for a chitosan-genipin system [89]. Therefore, it can be concluded that this peak is masked by collagen peaks in the same range. A secondary amide is also a characteristic of the collagen-genipin reaction and has a $C=O$ stretching vibration in the range $1680-1630$ cm^{-1}. However, since collagen's amide I and II peaks are in that range, it is not possible to quantify the increase in secondary amide groups after genipin crosslinking.
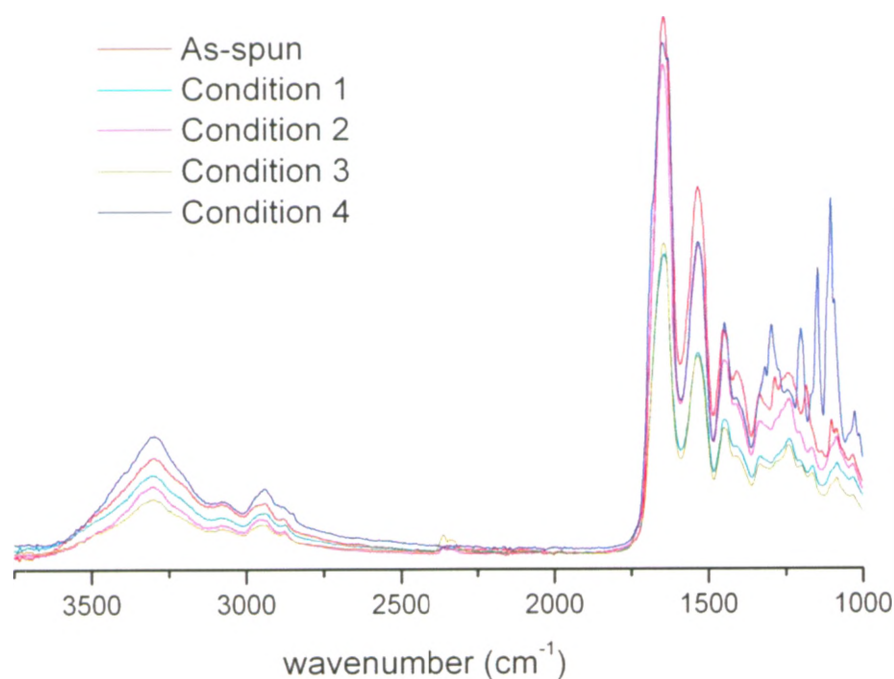
Figure 25. FTIR spectra of collagen nanofibers crosslinked using the four conditions and the as-spun fibers
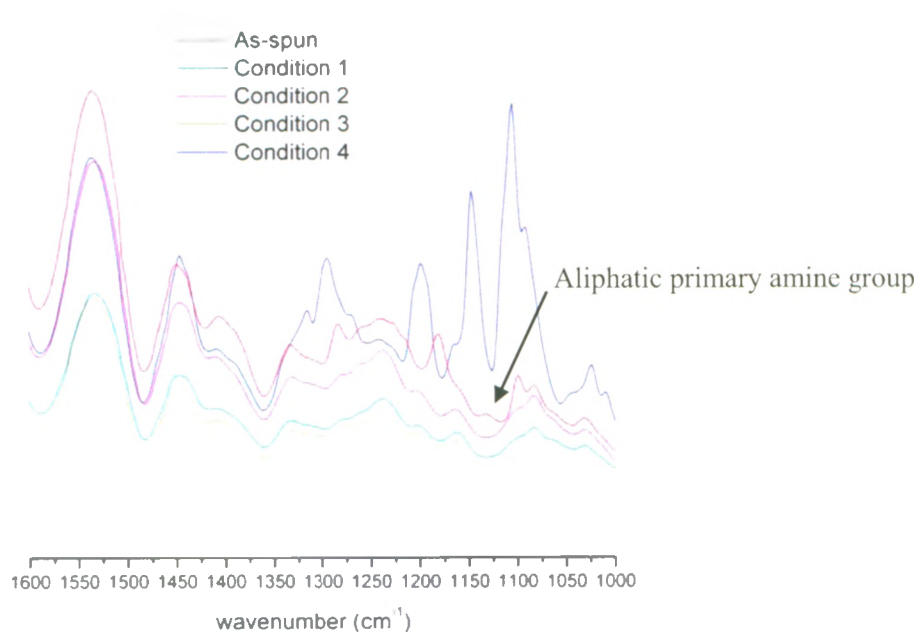
Figure 26. The C-N stretching vibration of a primary aliphatic amine with the structure (-CH-NH₂) shown at the absorption 1133 cm⁻¹

Crosslinking condition 4 yielded a different FTIR spectrum compared to the other three conditions. Figure 27 shows similar peaks between the genipin powder spectrum (Figure 24) and condition 4 samples, which used isopropanol as the crosslinking medium instead of ethanol. The following are the similar peaks between genipin and samples crosslinked using condition 4: 1105, 1147, 1200, 1298 and 1445 cm⁻¹. The appearance of those peaks confirms the availability of genipin molecules that are not fully reacted. Interestingly, it can be observed that the two peaks, 1298 and 1445 cm⁻¹, that represent the C-O-C asymmetric stretch and the CH₃ bend of the methyl ester respectively, are present in collagen samples crosslinked using condition 4. Therefore, it can be interpreted that the second crosslinking reaction (Figure 5) which takes place at the ester group is slowed down by isopropanol (i.e. isopropanol is slowing down the nucleophilic substitution that involves the replacement of the ester group on genipin by a secondary amide linkage).

4.7 Cellular attachment and morphology

Fibroblasts adhered to both the 2D collagen gel (uncrosslinked as-spun fibers exposed to growth media) and the 3D genipin-crosslinked collagen nanofibers. However, the difference in cellular morphology was evident from the fluorescence microscopy images shown in Figure 28. On the collagen gel the fibroblasts were spread out, had aggregated stress fibers, and had few extensions. Depending on whether the substrate is free floating or anchored to the cover slip, fibroblasts on the crosslinked samples acquired two different morphologies: a bipolar morphology or a neuron-like morphology with dendritic extensions.

Fibroblasts on the 2D collagen gels had similar morphology to those reported in the literature. Since the gels were fixed to the cover slip, the cells experienced isometric tension (internal and external mechanical forces balance such that cell contraction occurs without change in length [98]) and produced actin-aggregated fibers and were flattened (Figure 28A). Fibroblasts on 3D crosslinked collagen nanofibers, however, acquired a bipolar/stellate morphology when the samples were fixed to the cover slip (stressed), and acquired a dendrite-like structure when the samples were floating (unstressed). Figure 29A shows the dendritic morphology acquired by the fibroblasts when cultured on a floating sample crosslinked using condition 1, while Figure 29B shows the more spread, stellate morphology acquired by fibroblasts cultured on an anchored sample also crosslinked using condition 1. The dendritic morphology can be observed in samples crosslinked using condition 3, while more stellate morphologies can be observed in samples crosslinked using condition 2 (Figure 28C). Anchored samples crosslinked using condition 4 stimulated the fibroblasts to acquire a bipolar morphology (Figure 28E). It is important to mention, however, that most crosslinked samples did not fully adhere to the cover slip, since they were not fully dried on the cover slips, to avoid losing the 3D morphology due to surface tension effects caused by water evaporation.

Figure 30 shows the cell count on the collagen gels and all the genipin-crosslinked samples. Statistically there was no significant difference between the cell counts on the gels and on the crosslinked samples ($P > 0.05$). However, there was a significant difference between the samples crosslinked using condition 2, compared to conditions 3

and 4 (P<0.05). This difference in cell count amongst samples crosslinked using different conditions can give a preliminary insight into the conditions that are more cell-friendly.

Overall, it can be concluded from the cell-attachment studies and the cell counts between crosslinked samples and collagen gels, that the genipin-crosslinked collagen nanofibers support fibroblast attachment in the tested time period (24 hours). Also, the effect of stressed and unstressed substrates on the fibroblast morphology was in agreement with the literature.

	Primary human fibroblasts
As-spun collagen (i.e. collagen gel)	
Condition 1	
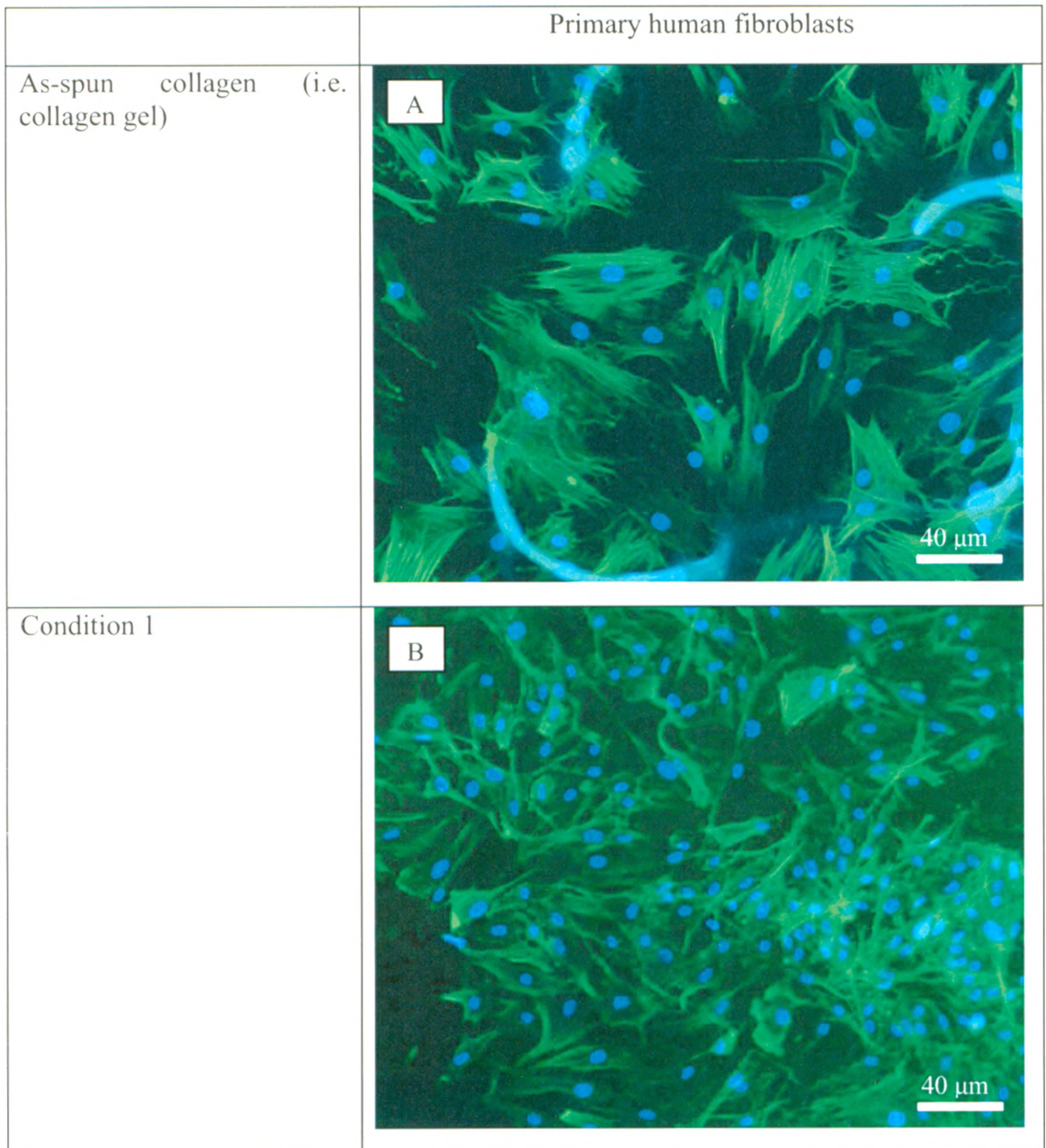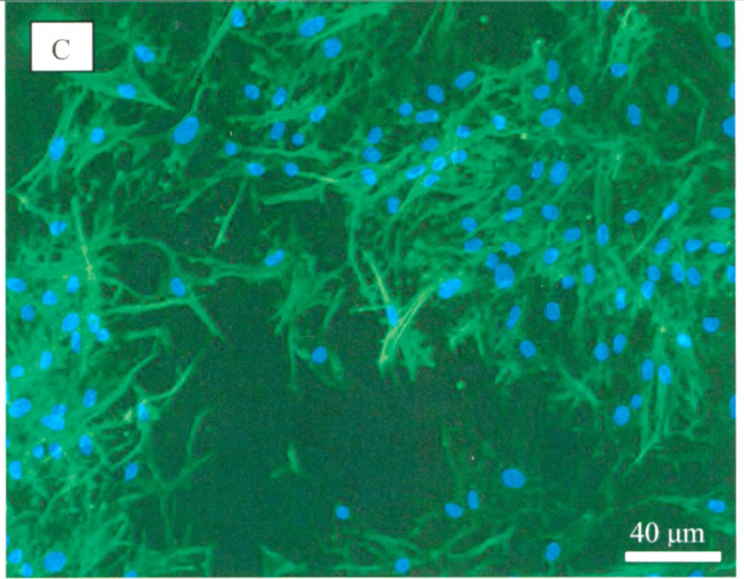
| Condition 2 | |
| Condition 3 | |
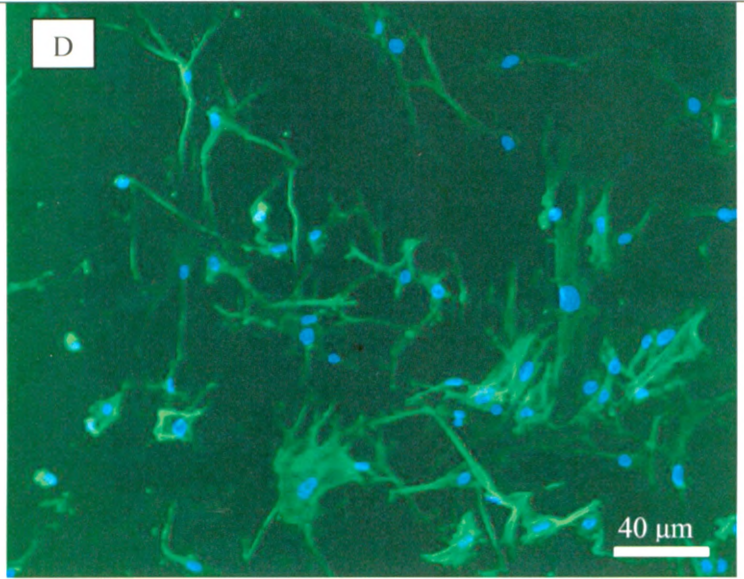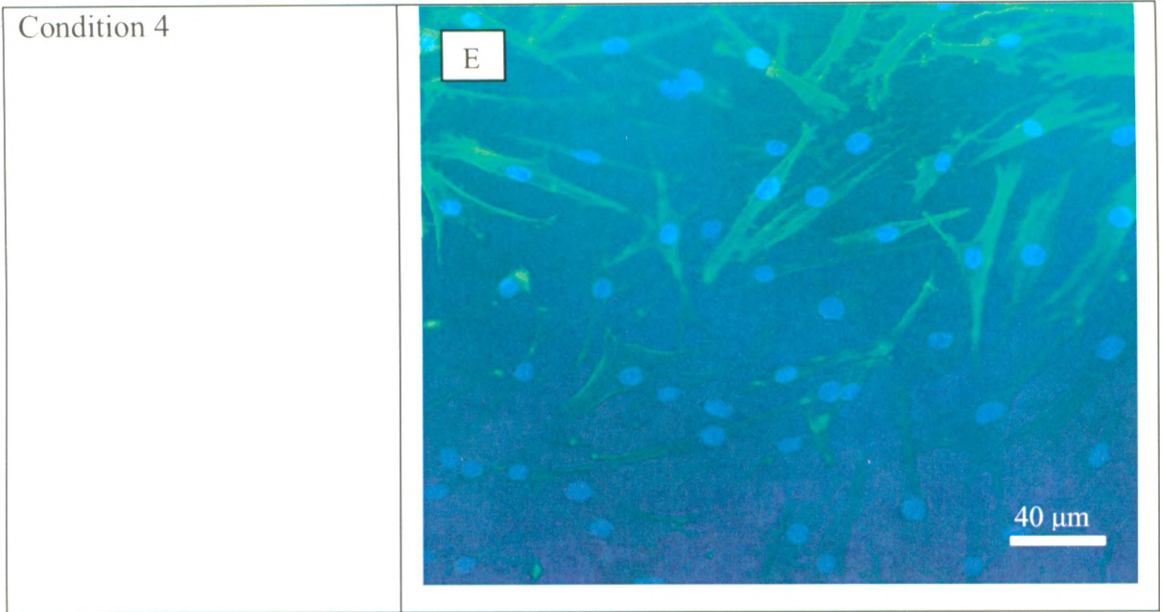
Figure 28. Fluorescence images of primary human fibroblasts cultured on a collagen gel (2D) and genipin-crosslinked collagen nanofibers (3D) using the four conditions (Fibroblasts were cultured on all samples for 24 hours prior to fixation and imaging)

Figure 29. Fluoresence images of primary human fibroblasts cultured on [A] floating and [B] anchored samples crosslinked using condition 1
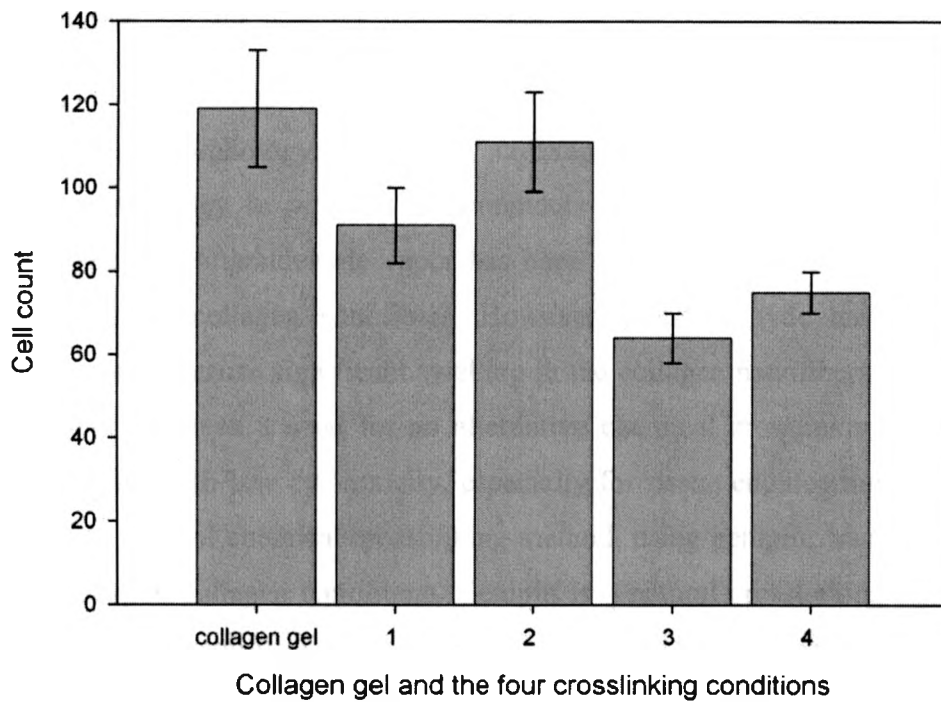
Figure 30. Cell counts carried out, after 24 hours of cell-seeding, on un-crosslinked collagen gels, and samples crosslinked using the 4 conditions (n=45)

5 Conclusion

As-spun collagen nanofibers swell significantly in aqueous environments and lose their nanofibrous morphology. Therefore, crosslinking is essential to preserve the nanofibrous morphology in aqueous environments and control their mechanical and swelling properties. Glutaraldehyde vapor has been used extensively, by most research groups, to crosslink collagen nanofibers. However, glutaraldehyde has been proven cytotoxic to cells and cause significant swelling in the collagen nanofibers after fixation. Therefore, there has been a need for an alternative chemical crosslinking method that yields stable fibers with low cytotoxicity, especially for tissue engineering applications. In this research, a novel chemical crosslinking method, using genipin, was introduced to stabilize electrospun collagen nanofibers. Genipin is a natural crosslinking agent which has been proven to be significantly less cytotoxic compared to glutaraldehyde.

Collagen nanofibers, with average fiber diameters of 171 ± 34 nm, have been successfully electrospun from rat tail collagen type I. Aligning the fibers was achieved using the 'two-electrodes' method as well as a rotating mandrel. Electrospun collagen nanofibers were successfully crosslinked using genipin. Crosslinking parameters that were investigated included: solvent (ethanol vs. isopropanol), water content (3% vs. 5%) and crosslinking duration (3 vs. 5 days). Four crosslinking conditions were developed based on the ability to stabilize the collagen nanofibers and allow for swelling control. The four crosslinking conditions were as follows: (1) ethanol, 5 % water and 3 days, (2) ethanol, 3% water and 5 days, (3) ethanol, 5% water and 5 days, and (4) isopropanol, 5% water and 5 days.

Two stages of swelling were studied: after crosslinking, and after exposure to growth media for 2, 5 and 7 days. It was observed that fibers crosslinked using conditions 1 and 3 had the most swelling after crosslinking (196 ± 8 % and 180 ± 7 %, respectively), as compared to conditions 2 and 4 (55 ± 5 % and 56 ± 4 %, respectively). This swelling was attributed to the higher water content used in conditions 1 and 3 (5 v/v %) as compared to condition 2 (3 v/v %). Morevoer, the higher hydrophobicity of isopropanol (used in condition 4) was responsible for the less fiber swelling compared to ethanol (used in condition 3).

In the second stage of swelling, condition 1 yielded no further swelling for up to 7 days in growth media, while condition 3 swelled for an additional 23% after 7 days in DMEM. The difference in swelling between conditions 1 and 3, was attributed to the increased formation of genipin oligomers with time; this oligomerisation lead to higher fiber porosity, and thus more swelling. After 7 days in growth media, condition 2 underwent a further 24% swelling, while condition 4, of all the conditions, underwent the highest degree of swelling (59%). The high degree of swelling, using condition 4, was attributed to the higher hydrophobicity of isopropanol, as compared to ethanol, which inhibited the completion of the crosslinking reaction of genipin molecules.

The ninhydrin assay was used to quantify the percentage of primary amine groups that reacted with genipin. Therefore, the assay was used as a method of quantifying the degree of crosslinking. However, the assay does not give information on the nature or density of crosslinking. Results showed that crosslinking condition 1 yielded the least degree of crosslinking as compared to the other conditions. Also, glutaraldehyde-crosslinked samples were tested, and the degree of crosslinking was comparable to all genipin-crosslinked samples, except condition 1. It was also observed that glutaraldehyde is a faster crosslinking method, since 24 hours of glutaraldehyde crosslinking was equivalent to 5 days of genipin crosslinking.

The effect of hydrolysis on the crosslinked nanofibers was tested using the ninhydrin assay to detect free amine groups that dissolved in water over the durations of 1, 3 and 7 days. It was observed that the amount of free amine groups detected in the water after 7 days was negligible for all 4 crosslinking conditions. Of all crosslinking conditions, condition 4 yielded the highest percent weight dissolved (0.3 ± 0.16 %).

Fourier-Transform Infrared spectroscopy was used to compare the chemical structures of as-spun collagen and genipin-crosslinked samples. All genipin-crosslinked samples shared the same infrared absorptions as the as-spun samples, except for a peak at 1133 cm^{-1} (attributed to a C-N stretching vibration of an aliphatic primary amine group) which disappeared after crosslinking. The resulting absence of this peak confirmed the reaction of primary amine groups with genipin molecules. Moreover, the FTIR of collagen samples crosslinked using condition 4, showed 4 peaks that were common to

absorption peaks of genipin powder (1105, 1147, 1200 and 1298 cm^{-1}). These shared absorption peaks confirmed the availability of non-fully reacted genipin molecules.

Cell-compatibility was tested by seeding the crosslinked samples with primary human fibroblasts that were acquired from the palmar fascia of the hand. Fluorescence microscopy images showed the attachment of cells to collagen gels (uncrosslinked, as-spun collagen fibers exposed to growth media), as well as to collagen nanofibers crosslinked using the 4 conditions. Samples that were not anchored to the cover slip resulted in cells that had dendritic-like extensions, while samples that were anchored resulted in cells with bipolar morphologies. These observations were consistent with the literature.

6 Future work

Research presented in this thesis lays the groundwork for a wide range of possibilities in the fields of skin, bone, cardiovascular, and neurological tissue engineering. Therefore, much work remains to be done in characterizing the chemical structures of the fibers as well as their mechanical properties. Moreover, extensive cell studies are required to examine cellular proliferation, differentiation and migration.

In terms of characterization, one of the most important experiments would be to measure the stiffness of individual crosslinked fibers using atomic force microscopy. Also, more studies are required to examine the chemical composition of these fibers using Raman spectroscopy and solid C^{13}-NMR. The degrees of crosslinking have to also be characterized using Differential Scanning Calorimetry (DSC), to better understand the crosslinking mechanism. Degradation of the fibers should be studied in more body-like conditions using the enzyme collagenase, in order to better predict the degree of degradation in the body.

Cell proliferation on these crosslinked fibers needs to be quantified if they were to be used in a tissue engineering application. However, a mechanism to fix the crosslinked samples to the cover slips is essential to allow cellular proliferation. In addition, the cellular differentiation could be controlled by chemically attaching growth factors to the nanofibers. Furthermore, different cell types, such as myofibroblasts and osteoblasts, could also be seeded and studied on the genipin-crosslinked collagen nanofibers.

Appendix A – Calibration curve for the ninhydrin assay

Glycine was chosen to calibrate the ninhydrin assay, as mentioned in the literature [79, 80, 104]. A 10 ml stock solution of glycine in distilled water (0.13 mg/ml) was first prepared. Five vials containing 5 ml of distilled water were also prepared. 5 ml of the stock solution was then transferred to the first vial and mixed well, thus reducing the glycine concentration by half (i.e. 0.065 mg/ml). 5 ml from first vial was then transferred to the second vial, diluting the concentration further; this process was repeated until the fifth vial (where 5 ml are disposed). This yielded 5 vials with the concentrations listed in Table A1. 1 ml of the ninhydrin solution was added to 2 ml of each of the five glycine concentrations and heated at 80°C for 15 minutes. The vials were then left to cool for 10 minutes and the absorbance was measured at 570 nm, using a UV spectrophotometer (Beckman DU series). At a concentration of 0.13 mg/ml, the absorbance was 3.109, which means the assay is not viable above a glycine concentration of 0.13 mg/ml.

Table A 1. Raw data for the ninhydrin calibration curve

Glycine concentration (mg/ml)	Absorbance at 570 nm
0.0650	3.108
0.0325	2.2420
0.0163	1.0150
0.0081	0.5700
0.0040	0.2390
0.0000	0.0000
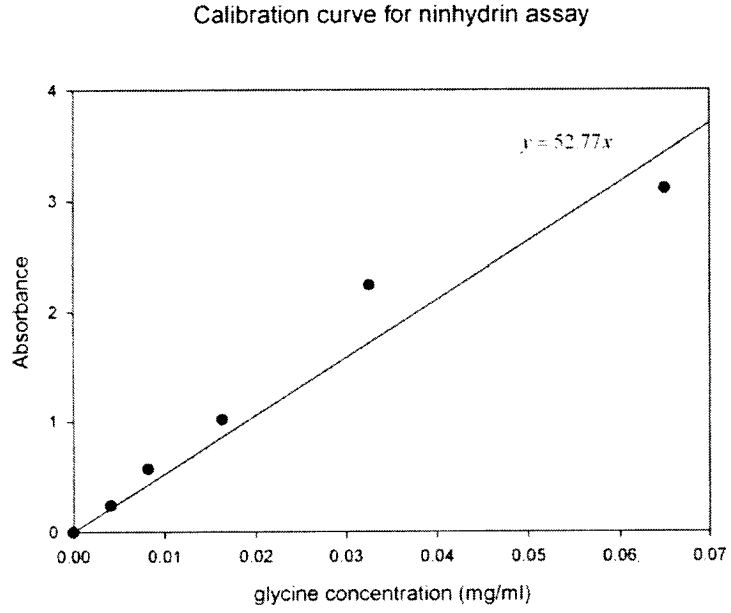
Figure A 1.Calibration curve for the ninhydrin assay using different glycine concentrations

Appendix B – Histograms for the genipin-crosslinked samples and after exposure to DMEM for 2 and 7 days

Crosslinking condition	Crosslinked	In DMEM for 2 days	In DMEM for 7 days
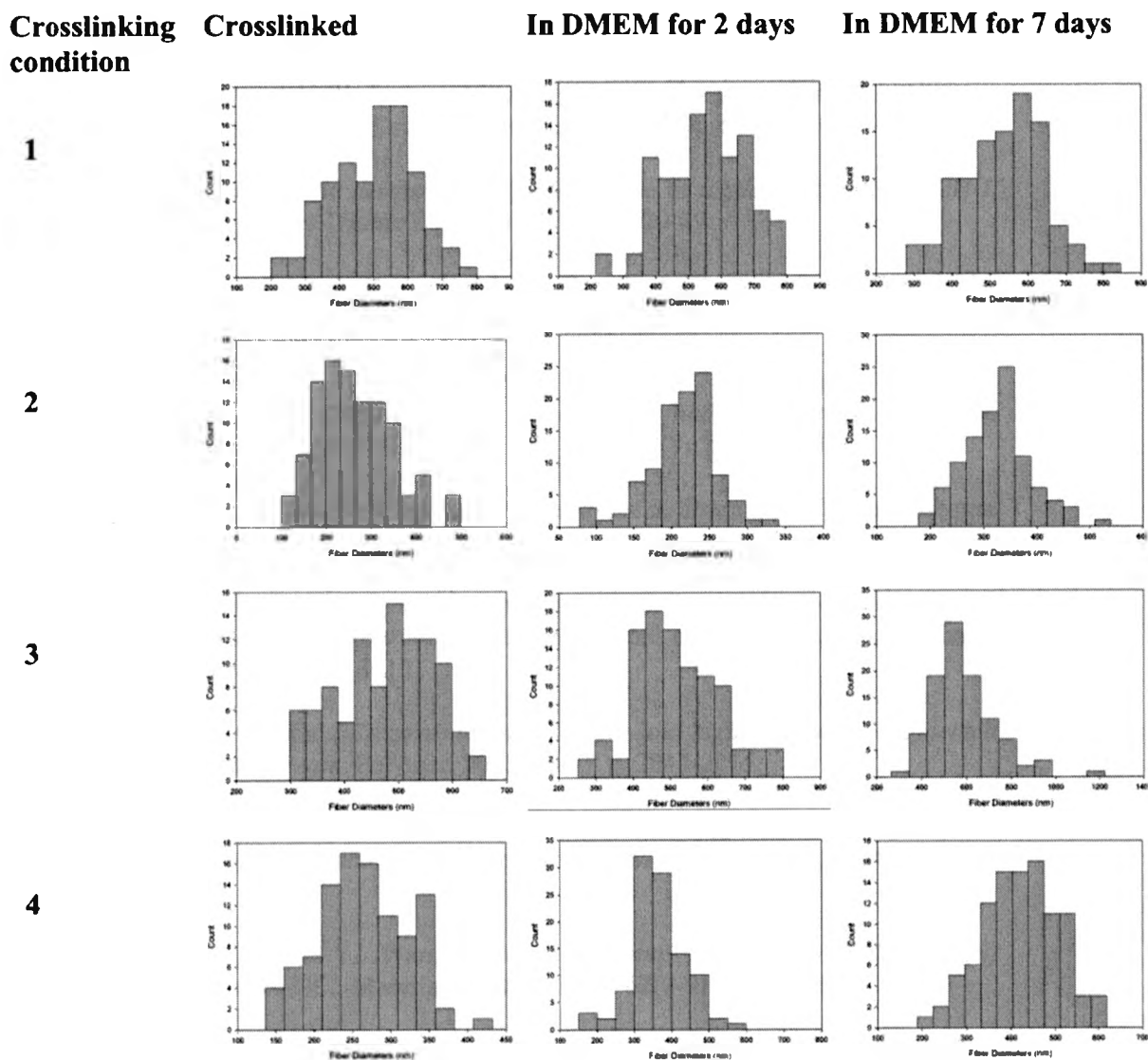
References

1. Nerem, R.M., *Tissue Engineering in the USA*. Medical & Biological Engineering & Computing, 1992. **30**(4): p. Ce8-Ce12.

2. Vacanti, C.A., *History of tissue engineering and a glimpse into its future*. Tissue Eng, 2006. **12**(5): p. 1137-42.

3. Dang, J.M. and K.W. Leong, *Natural polymers for gene delivery and tissue engineering*. Advanced Drug Delivery Reviews, 2006. **58**(4): p. 487-499.

4. Yang, S., et al., *The design of scaffolds for use in tissue engineering. Part I. Traditional factors*. Tissue Eng, 2001. **7**(6): p. 679-89.

5. Seeram Ramakrishna, K.F., Wee-Eong Teo, Teik-Cheng Lim and Zuwei Ma, *Electrospinning and Nanofibers*. 2005: Singapore: World Scientific Publishing Co. Pte. Ltd.

6. Shin, Y.M., et al., *Electrospinning: A whipping fluid jet generates submicron polymer fibers*. Applied Physics Letters, 2001. **78**(8): p. 1149-1151.

7. Subbiah, T., et al., *Electrospinning of nanofibers*. Journal of Applied Polymer Science, 2005. **96**(2): p. 557-569.

8. Cui, W.G., et al., *Investigation on process parameters of electrospinning system through orthogonal experimental design*. Journal of Applied Polymer Science, 2007. **103**(5): p. 3105-3112.

9. McKee, M.G., et al., *Electrospinning of linear and highly branched segmented poly(urethane urea)s*. Polymer, 2005. **46**(7): p. 2011-2015.

10. McKee, M.G., et al., *Correlations of solution rheology with electrospun fiber formation of linear and branched polyesters*. Macromolecules, 2004. **37**(5): p. 1760-1767.

11. Qin, X.H. and S.Y. Wang, *Interior structure of polyacrylonitrile(PAN) nanofibers with LiCl*. Materials Letters, 2008. **62**(8-9): p. 1325-1327.

12. Arayanarakul, K., et al., *Effects of poly(ethylene glycol), inorganic salt, sodium dodecyl sulfate, and solvent system on electrospinning of poly(ethylene oxide)*. Macromolecular Materials and Engineering, 2006. **291**(6): p. 581-591.

13. Deitzel, J.M., et al., *The effect of processing variables on the morphology of electrospun nanofibers and textiles*. Polymer, 2001. **42**(1): p. 261-272.

14. Zong, X.H., et al., *Structure and process relationship of electrospun bioabsorbable nanofiber membranes*. Polymer, 2002. **43**(16): p. 4403-4412.

15. Nair, L.S., et al., *Fabrication and optimization of methylphenoxy substituted polyphosphazene nanofibers for biomedical applications*. Biomacromolecules, 2004. **5**(6): p. 2212-2220.

16.   Megelski, S., et al., *Micro- and nanostructured surface morphology on electrospun polymer fibers.* Macromolecules, 2002. **35**(22): p. 8456-8466.

17.   Ojha, S.S., et al., *Morphology of electrospun nylon-6 nanofibers as a function of molecular weight and processing parameters.* Journal of Applied Polymer Science, 2008. **108**(1): p. 308-319.

18.   Hong, Y.L., et al., *Synthesis using electrospinning and stabilization of single layer macroporous films and fibrous networks of poly(vinyl alcohol).* Journal of Membrane Science, 2006. **276**(1-2): p. 1-7.

19.   Katti, D.S., et al., *Bioresorbable nanofiber-based systems for wound healing and drug delivery: Optimization of fabrication parameters.* Journal of Biomedical Materials Research Part B-Applied Biomaterials, 2004. **70B**(2): p. 286-296.

20.   Matthews, J.A., et al., *Electrospinning of collagen nanofibers.* Biomacromolecules, 2002. **3**(2): p. 232-238.

21.   Theron, A., E. Zussman, and A.L. Yarin, *Electrostatic field-assisted alignment of electrospun nanofibres.* Nanotechnology, 2001. **12**(3): p. 384-390.

22.   Li, D., Y.L. Wang, and Y.N. Xia, *Electrospinning of polymeric and ceramic nanofibers as uniaxially aligned arrays.* Nano Letters, 2003. **3**(8): p. 1167-1171.

23.   Yao, L., *Electrospinning of poly(vinyl alcohol) nanofibers.* Abstracts of Papers of the American Chemical Society, 2002. **223**: p. U631-U631.

24.   Jia, Z.D., et al., *Preparation and properties of poly (vinyl alcohol) nanofibers by electrospinning.* Journal of Polymer Engineering, 2008. **28**(1-2): p. 87-100.

25.   Osanai, Y., O.H. Kwon, and H. Uyama, *Preparation of rapidly degradable poly(L-lactic acid) nanofiber non-woven mat via electrospinning.* Abstracts of Papers of the American Chemical Society, 2005. **229**: p. U946-U946.

26.   Inai, R., M. Kotaki, and S. Ramakrishna, *Structure and properties of electrospun PLLA single nanofibres.* Nanotechnology, 2005. **16**(2): p. 208-213.

27.   Zong, X.H., et al., *Electrospun fine-textured scaffolds for heart tissue constructs.* Biomaterials, 2005. **26**(26): p. 5330-5338.

28.   Bini, T.B., et al., *Electrospun poly(L-lactide-co-glycolide) biodegradable polymer nanofibre tubes for peripheral nerve regeneration.* Nanotechnology, 2004. **15**(11): p. 1459-1464.

29.   Khil, M.S., et al., *Electrospun nanofibrous polyurethane membrane as wound dressing.* Journal of Biomedical Materials Research Part B-Applied Biomaterials, 2003. **67B**(2): p. 675-679.

30.   Yoshimoto, H., et al., *A biodegradable nanofiber scaffold by electrospinning and its potential for bone tissue engineering.* Biomaterials, 2003. **24**(12): p. 2077-2082.

31.   Li, W.J., et al., *A three-dimensional nanofibrous scaffold for cartilage tissue engineering using human mesenchymal stem cells.* Biomaterials, 2005. **26**(6): p. 599-609.

32.   Ki, C.S., et al., *Characterization of gelatin nanofiber prepared from gelatin-formic acid solution.* Polymer, 2005. **46**(14): p. 5094-5102.

33.   Huang, Z.M., et al., *Electrospinning and mechanical characterization of gelatin nanofibers.* Polymer, 2004. **45**(15): p. 5361-5368.

34.   Meng, W., et al., *Electrospun PHBV/collagen composite nanofibrous scaffolds for tissue engineering.* Journal of Biomaterials Science-Polymer Edition, 2007. **18**(1): p. 81-94.

35.   Rho, K.S., et al., *Electrospinning of collagen nanofibers: Effects on the behavior of normal human keratinocytes and early-stage wound healing.* Biomaterials, 2006. **27**(8): p. 1452-1461.

36.   Yang, L., et al., *Mechanical properties of single electrospun collagen type I fibers.* Biomaterials, 2008. **29**(8): p. 955-962.

37.   Zhong, S.P., et al., *An aligned nanofibrous collagen scaffold by electrospinning and its effects on in vitro fibroblast culture.* Journal of Biomedical Materials Research Part A, 2006. **79A**(3): p. 456-463.

38.   Matthews, J.A., et al., *Electrospinning of collagen type II: A feasibility study.* Journal of Bioactive and Compatible Polymers, 2003. **18**(2): p. 125-134.

39.   Ohkawa, K., et al., *Electrospinning of chitosan.* Macromolecular Rapid Communications, 2004. **25**(18): p. 1600-1605.

40.   Geng, X.Y., O.H. Kwon, and J.H. Jang, *Electrospinning of chitosan dissolved in concentrated acetic acid solution.* Biomaterials, 2005. **26**(27): p. 5427-5432.

41.   Um, I.C., et al., *Electro-spinning and electro-blowing of hyaluronic acid.* Biomacromolecules, 2004. **5**(4): p. 1428-1436.

42.   Ji, Y., et al., *Electrospun three-dimensional hyaluronic acid nanofibrous scaffolds.* Biomaterials, 2006. **27**(20): p. 3782-3792.

43.   Zhang, Y.Z., et al., *Electrospinning of gelatin fibers and gelatin/PCL composite fibrous scaffolds.* Journal of Biomedical Materials Research Part B-Applied Biomaterials, 2005. **72B**(1): p. 156-165.

44.   Duan, B., et al., *Electrospinning of chitosan solutions in acetic acid with poly(ethylene oxide).* Journal of Biomaterials Science-Polymer Edition, 2004. **15**(6): p. 797-811.

45.   Huang, L., et al., *Engineered collagen-PEO nanofibers and fabrics.* Journal of Biomaterials Science-Polymer Edition, 2001. **12**(9): p. 979-993.

46.   Li, J.X., et al., *Electrospinning of hyaluronic acid (HA) and HA/gelatin blends.* Macromolecular Rapid Communications, 2006. **27**(2): p. 114-120.

47.   Chen, Z.G., X.M. Mo, and F.L. Qing, *Electrospinning of collagen-chitosan complex.* Materials Letters, 2007. **61**(16): p. 3490-3494.

48.   Brinckmann, J., *Collagens at a glance.* Collagen, 2005. **247**: p. 1-6.

49.   Woodhead, J., *Collagen: the Anatomy of a Protein.* Studies in Biology no.117, ed. T.i.o.B.s.s.i. biology. 1980: Edward Arnold.

50.   Nimni, M.E., *Collagen.* Collagen-Biochemistry, ed. M.E. Nimni. Vol. 1. 1988: Library of Congree Cataloging-in-Publication Data (CRC Press).

51.   Vanderrest, M. and R. Garrone, *Collagen Family of Proteins.* Faseb Journal, 1991. **5**(13): p. 2814-2823.

52.   Miller, E.J., *Isolation and Characterization of a Collagen from Chick Cartilage Containing 3 Identical Alpha-Chains.* Biochemistry, 1971. **10**(9): p. 1652-&.

53.   Miller, E.J. and V.J. Matukas, *Chick Cartilage Collagen . A New Type of Alpha1 Chain Not Present in Bone or Skin of Species.* Proceedings of the National Academy of Sciences of the United States of America, 1969. **64**(4): p. 1264-&.

54.   Kefalide.Na, *Isolation of a Collagen from Basement Membranes Containing 3 Identical Alpha-Chains.* Biochemical and Biophysical Research Communications, 1971. **45**(1): p. 226-&.

55.   Petruska, J.A. and A.J. Hodge, *A Subunit Model for the Tropocollagen Macromolecule.* Proc Natl Acad Sci U S A, 1964. **51**: p. 871-6.

56.   Bhattacharjee, A. and M. Bansal, *Collagen structure: The Madras triple helix and the current scenario.* Iubmb Life, 2005. **57**(3): p. 161-172.

57.   Ramachandran, G.N. and G. Kartha, *Structure of collagen.* Nature, 1954. **174**(4423): p. 269-70.

58.   Nordwig, K.H.a.A., *Amino acid sequences in collagen*, in *Treatise on Collagen*, G.N. Ramachandran, Editor. 1967, Academic Press.

59.   Ramachandran, G.N., *Elements of the Helical structure of collagen.* Current Science, 1954. **23**: p. 349-350.

60.   Ramachandran, G.N., *Structure of collagen at the molecular level*, in *Treatise on Collagen*, G.N. Ramachandran, Editor. 1967, Academic press. p. 103-183.

61.   Birk, D.E. and P. Bruckner, *Collagen suprastructures.* Collagen, 2005. **247**: p. 185-205.

62.   Hodge, A.J., *Structure at the Electron Microscopic level*, in *Treatise on Collagen*, G.N. Ramachandran, Editor. 1967, Academic press. p. 185 - 205.

63.   Smith, J.W., *Molecular pattern in native collagen.* Nature, 1968. **219**(5150): p. 157-8.

64.   Piez, K.A. and B.L. Trus, *A new model for packing of type-I collagen molecules in the native fibril.* Biosci Rep, 1981. **1**(10): p. 801-10.

65.   van Zuijlen, P.P.M., et al., *Collagen morphology in human skin and scar tissue: no adaptations in response to mechanical loading at joints.* Burns, 2003. **29**(5): p. 423-431.

66.   Komuro, T., *The Lattice Arrangement of the Collagen-Fibers in the Submucosa of the Rat Small-Intestine - Scanning Electron-Microscopy.* Cell and Tissue Research, 1988. **251**(1): p. 117-121.

67.   Lo, D. and I. Vesely, *Biaxial strain analysis of the porcine aortic valve.* Ann Thorac Surg, 1995. **60**(2 Suppl): p. S374-8.

68.   Kleinman, H.K., et al., *Localization of Binding-Site for Cell Attachment in Alpha-1(I) Chain of Collagen.* Journal of Biological Chemistry, 1978. **253**(16): p. 5642-5656.

69.   Pankov, R. and K.M. Yamada, *Fibronectin at a glance.* Journal of Cell Science, 2002. **115**(20): p. 3861-3863.

70.   Li, M.Y., et al., *Electrospun protein fibers as matrices for tissue engineering.* Biomaterials, 2005. **26**(30): p. 5999-6008.

71.   Huanglee, L.L.H., D.T. Cheung, and M.E. Nimni, *Biochemical-Changes and Cytotoxicity Associated with the Degradation of Polymeric Glutaraldehyde Derived Cross-Links.* Journal of Biomedical Materials Research, 1990. **24**(9): p. 1185-1201.

72.   Gough, J.E., C.A. Scotchford, and S. Downes, *Cytotoxicity of glutaraldehyde crosslinked collagen/poly(vinyl alcohol) films is by the mechanism of apoptosis.* Journal of Biomedical Materials Research, 2002. **61**(1): p. 121-130.

73.   Maizato, M.J., et al., *Glutaraldehyde-treated bovine pericardium: effects of lyophilization on cytotoxicity and residual aldehydes.* Artif Organs, 2003. **27**(8): p. 692-4.

74.   Speit, G., et al., *The genotoxic potential of glutaraldehyde in mammalian cells in vitro in comparison with formaldehyde.* Mutation Research-Genetic Toxicology and Environmental Mutagenesis, 2008. **649**(1-2): p. 146-154.

75.   Gendler, E., S. Gendler, and M.E. Nimni, *Toxic Reactions Evoked by Glutaraldehyde-Fixed Pericardium and Cardiac-Valve Tissue Bioprosthesis.* Journal of Biomedical Materials Research, 1984. **18**(7): p. 727-736.

76.   Barnes, C.P., et al., *Cross-linking electrospun type II collagen tissue engineering scaffolds with carbodiimide in ethanol.* Tissue Engineering, 2007. **13**(7): p. 1593-1605.

77.   Buttafoco, L., et al., *Electrospinning of collagen and elastin for tissue engineering applications.* Biomaterials, 2006. **27**(5): p. 724-734.

78.   Park, J.E., et al., *Isolation and characterization of water-soluble intermediates of blue pigments transformed from geniposide of Gardenia jasminoides.* Journal of Agricultural and Food Chemistry, 2002. **50**(22): p. 6511-6514.

79.   Sung, H.W., et al., *Crosslinking characteristics and mechanical properties of a bovine pericardium fixed with a naturally occurring crosslinking agent.* Journal of Biomedical Materials Research, 1999. **47**(2): p. 116-126.

80.   Sung, H.W., et al., *Mechanical properties of a porcine aortic valve fixed with a naturally occurring crosslinking agent.* Biomaterials, 1999. **20**(19): p. 1759-1772.

81.   Sung, H.W., et al., *In vitro evaluation of cytotoxicity of a naturally occurring cross-linking reagent for biological tissue fixation.* Journal of Biomaterials Science-Polymer Edition, 1999. **10**(1): p. 63-78.

82.   Huang, L.L.H., et al., *Biocompatibility study of a biological tissue fixed with a naturally occurring crosslinking reagent.* Journal of Biomedical Materials Research, 1998. **42**(4): p. 568-576.

83.   Tsai, C.C., et al., *In vitro evaluation of the genotoxicity of a naturally occurring crosslinking agent (genipin) for biologic tissue fixation.* Journal of Biomedical Materials Research, 2000. **52**(1): p. 58-65.

84.   Chang, Y., et al., *In vivo evaluation of cellular and acellular bovine pericardia fixed with a naturally occurring crosslinking agent (genipin).* Biomaterials, 2002. **23**(12): p. 2447-2457.

85.   Touyama, R., et al., *Studies on the Blue Pigments Produced from Genipin and Methylamine .2. On the Formation Mechanisms of Brownish-Red Intermediates Leading to the Blue Pigment Formation.* Chemical & Pharmaceutical Bulletin, 1994. **42**(8): p. 1571-1578.

86.   Touyama, R., et al., *Studies on the Blue Pigments Produced from Genipin and Methylamine .1. Structures of the Brownish-Red Pigments, Intermediates Leading to the Blue Pigments.* Chemical & Pharmaceutical Bulletin, 1994. **42**(3): p. 668-673.

87. Paik, Y.S., et al., *Physical stability of the blue pigments formed from geniposide of gardenia fruits: Effects of pH, temperature, and light.* Journal of Agricultural and Food Chemistry, 2001. **49**(1): p. 430-432.

88. Butler, M.F., Y.F. Ng, and P.D.A. Pudney, *Mechanism and kinetics of the crosslinking reaction between biopolymers containing primary amine groups and genipin.* Journal of Polymer Science Part a-Polymer Chemistry, 2003. **41**(24): p. 3941-3953.

89. Mi, F.L., H.W. Sung, and S.S. Shyu, *Synthesis and characterization of a novel chitosan-based network prepared using naturally occurring crosslinker.* Journal of Polymer Science Part a-Polymer Chemistry, 2000. **38**(15): p. 2804-2814.

90. Mi, F.L., S.S. Shyu, and C.K. Peng, *Characterization of ring-opening polymerization of genipin and pH-dependent cross-linking reactions between chitosan and genipin.* Journal of Polymer Science Part a-Polymer Chemistry, 2005. **43**(10): p. 1985-2000.

91. Hay, E.D., *The mesenchymal cell, its role in the embryo, and the remarkable signaling mechanisms that create it.* Dev Dyn, 2005. **233**(3): p. 706-720.

92. Doljanski, F., *The sculpturing role of fibroblast-like cells in morphogenesis.* Perspectives in Biology and Medicine, 2004. **47**(3): p. 339-356.

93. Lowe, A.S.a.J., *Human Histology.* Third Edition ed. 2005: Elsevier Limited.

94. Cukierman, E., R. Pankov, and K.M. Yamada, *Cell interactions with three-dimensional matrices.* Curr Opin Cell Biol, 2002. **14**(5): p. 633-9.

95. Grinnell, F., et al., *Dendritic fibroblasts in three-dimensional collagen matrices.* Molecular Biology of the Cell, 2003. **14**(2): p. 384-395.

96. Rhee, S. and F. Grinnell, *Fibroblast mechanics in 3D collagen matrices.* Adv Drug Deliv Rev, 2007. **59**(13): p. 1299-305.

97. Lauffenburger, D.A. and A.F. Horwitz, *Cell migration: a physically integrated molecular process.* Cell, 1996. **84**(3): p. 359-69.

98. Grinnell, F., *Fibroblast biology in three-dimensional collagen matrices.* Trends in Cell Biology, 2003. **13**(5): p. 264-269.

99. Cukierman, E., et al., *Taking cell-matrix adhesions to the third dimension.* Science, 2001. **294**(5547): p. 1708-1712.

100. Beertsen, W., C.A.G. McCulloch, and J. Sodek, *The periodontal ligament: A unique, multifunctional connective tissue.* Periodontology 2000, 1997. **13**: p. 20-40.

101. Breathnach, A.S., *Development and Differentiation of Dermal Cells in Man.* Journal of Investigative Dermatology, 1978. **71**(1): p. 2-8.

102.   Tamariz, E. and F. Grinnell, *Modulation of fibroblast morphology and adhesion during collagen matrix remodeling.* Molecular Biology of the Cell, 2002. **13**(11): p. 3915-3929.

103.   Fringer, J. and F. Grinnell, *Fibroblast quiescence in floating or released collagen matrices: contribution of the ERK signaling pathway and actin cytoskeletal organization.* J Biol Chem, 2001. **276**(33): p. 31047-52.

104.   Sung, H.W., et al., *Crosslinking of biological tissues using genipin and/or carbodiimide.* Journal of Biomedical Materials Research Part A, 2003. **64A**(3): p. 427-438.

105.   Howard, J.C., et al., *Wound healing-associated proteins Hsp47 and fibronectin are elevated in Dupuytren's contracture.* J Surg Res, 2004. **117**(2): p. 232-8.

106.   Starcher, B., *A ninhydrin-based assay to quantitate the total protein content of tissue samples.* Analytical Biochemistry, 2001. **292**(1): p. 125-129.

107.   Verreck, G., et al., *Incorporation of drugs in an amorphous state into electrospun nanofibers composed of a water-insoluble, nonbiodegradable polymer.* Journal of Controlled Release, 2003. **92**(3): p. 349-360.

108.   Zeng, J., et al., *Biodegradable electrospun fibers for drug delivery.* J Control Release, 2003. **92**(3): p. 227-31.

109.   Song, J.H., H.E. Kim, and H.W. Kim, *Production of electrospun gelatin nanofiber by water-based co-solvent approach.* Journal of Materials Science-Materials in Medicine, 2008. **19**(1): p. 95-102.

110.   Lin, Y.K. and D.C. Liu, *Comparison of physical-chemical properties of type I collagen from different species.* Food Chemistry, 2006. **99**(2): p. 244-251.

111.   Chew, S.Y., et al., *The effect of the alignment of electrospun fibrous scaffolds on Schwann cell maturation.* Biomaterials, 2008. **29**(6): p. 653-661.

112.   Chew, S.Y., et al., *Aligned protein-polymer composite fibers enhance nerve regeneration: A potential tissue-engineering platform.* Advanced Functional Materials, 2007. **17**(8): p. 1288-1296.

113.   Corey, J.M., et al., *Aligned electrospun nanofibers specify the direction of dorsal root ganglia neurite growth.* Journal of Biomedical Materials Research Part A, 2007. **83A**(3): p. 636-645.

114.   Nerurkar, N.L., D.M. Elliott, and R.L. Mauck, *Mechanics of oriented electrospun nanofibrous scaffolds for annulus fibrosus tissue engineering.* Journal of Orthopaedic Research, 2007. **25**(8): p. 1018-1028.

115.   Chiono, V., et al., *Genipin-crosslinked chitosan/gelatin blends for biomedical applications.* J Mater Sci Mater Med, 2008. **19**(2): p. 889-98.

116.   Chang, W.H., et al., *A genipin-crosslinked gelatin membrane as wound-dressing material: in vitro and in vivo studies*. J Biomater Sci Polym Ed, 2003. **14**(5): p. 481-95.

117.   Sung, H.W., et al., *Fixation of biological tissues with a naturally occurring crosslinking agent: fixation rate and effects of pH, temperature, and initial fixative concentration*. J Biomed Mater Res, 2000. **52**(1): p. 77-87.

118.   Ozaki, Y., A. Mizuno, and F. Kaneuchi, *Structural Differences between Type-I and Type-Iv Collagen in Biological Tissues Studied Invivo by Attenuated Total Reflection Fourier-Transform Infrared-Spectroscopy*. Applied Spectroscopy, 1992. **46**(4): p. 626-630.

119.   Petibois, C., et al., *Analysis of type I and IV collagens by FT-IR spectroscopy and imaging for a molecular investigation of skeletal muscle connective tissue*. Analytical and Bioanalytical Chemistry, 2006. **386**(7-8): p. 1961-1966.

120.   Socrates, G., *Infrared Characteristic Group Frequencies - Tables and Charts*. Second Edition ed. 1994: John Wiley and Sons.

121.   Sundararaghavan, H.G., et al., *Genipin-induced changes in collagen gels: Correlation of mechanical properties to fluorescence*. Journal of Biomedical Materials Research Part A, 2008. **87A**(2): p. 308-320.